

Neutral Higgs decays $H \rightarrow Z\gamma, \gamma\gamma$ in 3-3-1 models

H. T. Hung,^{1,*} T. T. Hong,^{2,1,†} H. H. Phuong,^{1,‡} H. L. T. Mai,^{3,§} and L. T. Hue^{¶4,5,**}

¹*Department of Physics, Hanoi Pedagogical University 2,*

Phuc Yen, Vinh Phuc 280000, Vietnam

²*Department of Physics, An Giang University,*

Ung Van Khiem Street, Long Xuyen, An Giang 880000, Vietnam

³*Faculty of Physics Science, Can Tho Medical College,*

Nguyen Van Cu Street, Can Tho 900000, Vietnam

⁴*Institute of Research and Development,*

Duy Tan University, Da Nang 550000, Vietnam

⁵*Institute of Physics, Vietnam Academy of Science and Technology,*

10 Dao Tan, Ba Dinh, Hanoi 100000, Vietnam

Abstract

The significance of new physics appearing in the loop-induced decays of neutral Higgs bosons into pairs of di-bosons $\gamma\gamma$ and $Z\gamma$ will be discussed in the framework of the 3-3-1 models based on a recent work [1], where the Higgs sector becomes effectively the same as that in the Two Higgs Doublet models (2HDM) after the first symmetry breaking from $SU(3)_L$ scale into the electroweak scale. For large $SU(3)_L$ scale $v_3 \simeq 10$ TeV, dominant one-loop contributions to the two decay amplitudes arise from only the single charged Higgs boson predicted by the 2HDM, leading to that experimental constraint on the signal strength $\mu_{\gamma\gamma}^{331}$ of the Standard model like Higgs boson decay $h \rightarrow \gamma\gamma$ will result in a strict upper bound on the signal strength $\mu_{Z\gamma}^{331}$ of the decay $h \rightarrow Z\gamma$. For a particular model with lower v_3 around 3 TeV, contributions from heavy charged gauge and Higgs bosons may have the same order, therefore may give strong destructive or constructive correlations. As a by product, deviations from the SM prediction $|\mu_{\gamma\gamma}^{331} - 1| \leq 0.04$ still allows $|\mu_{Z\gamma}^{331} - 1|$ to reach values near 0.1. We also show that there exists an CP-even neutral Higgs boson h_3^0 predicted by the 3-3-1 models, but beyond the 2HDM, has an interesting property that the branching ratio $\text{Br}(h_3^0 \rightarrow \gamma\gamma)$ is very sensitive to the parameter β used to distinguish different 3-3-1 models.

[¶] Corresponding author

*Electronic address: hathanhhung@hpu2.edu.vn

[†]Electronic address: tthong@agu.edu.vn

[‡]Electronic address: trongnghia.hd@gmail.com

[§]Electronic address: huynhmaict1509@gmail.com

^{**}Electronic address: lt hue@iop.vast.ac.vn

I. INTRODUCTION

One of the most important channels confirming the existence of the standard model-like (SM-like) Higgs boson is the loop-induced decay channel $h \rightarrow \gamma\gamma$. Experimentally, the respective signal strength has been updated recently by ATLAS and CMS [2–4]. There is another loop-induced decay $h \rightarrow Z\gamma$, which the branching ratio (Br) predicted by the standard model (SM) is $\text{Br}(h \rightarrow Z\gamma) = 1.54 \times 10^{-3} \pm 5.7\%$ corresponding to the Higgs boson mass $m_h = 125.09$ GeV [5, 6]. This decay channel has not been observed experimentally. The recent upper constraints of the signal strength are $\mu_{Z\gamma} < 6.6$ and $\mu_{Z\gamma} < 3.9$ from ATLAS and CMS [7, 8], respectively. In the future project from LHC with its High Luminosity (HL-LHC) and High Energy (HE-LHC), precision measurements for the signal strengths of the two decays $h \rightarrow Z\gamma$ and $h \rightarrow \gamma\gamma$ can reach the respective values of $\mu_{Z\gamma} = 1 \pm 0.23$ and $\mu_{\gamma\gamma} = 1 \pm 0.04$ for both ATLAS and CMS [9]. In addition, the ATLAS expected significance to the $h \rightarrow Z\gamma$ channel is hoped to be 4.9σ with 3000 fb^{-1} .

In theoretical side, the loop-induced decays of the SM-like Higgs boson mentioned above are important for searching as well as constraining new physics predicted by recent SM extensions, which are constructed to explain various current experiment data beyond the SM predictions. In the SM, leading contributions to the amplitudes of both decays $h \rightarrow \gamma\gamma, Z\gamma$ are at the one-loop level and relate with W and fermion mediation. On the other hand, SM extensions usually contain new charged particles including scalar, fermions, and gauge bosons spin 1. If any of them couple with the SM-like Higgs boson, they will contribute to the decay amplitude $h \rightarrow \gamma\gamma$ from the one-loop level. Normally, these particles also couple with the SM gauge boson Z , hence give one-loop contributions to the decay amplitude $h \rightarrow Z\gamma$ too. It seems that the Br of the two decays $h \rightarrow \gamma\gamma, Z\gamma$ have certain relations that the recent experimental constraint of $\mu_{\gamma\gamma}$ may result in a respective constraint on $\mu_{Z\gamma}$.

The theoretical studies of loop effects caused by new particles on the SM-like Higgs decays including $h \rightarrow \gamma\gamma, Z\gamma$ have been done recently in many SM extensions such as 2HDM [10, 11], where a thorough investigation in ref. [10] concerned strong correlations between two signal strengths $\mu_{\gamma\gamma, Z\gamma}$. Hence, the experimental data of $\mu_{\gamma\gamma}$ can be used as an efficient way to predict theoretically constraints on the $\mu_{Z\gamma}$. In the left-right model, the $h \rightarrow \gamma\gamma$ can be used as an approach to constraint the heavy charged gauge boson masses [12]. While, it seems that the old result of the decay $h \rightarrow Z\gamma$ [13, 14] has not been updated. In a recent

scotogenic model, new singly and doubly charged Higgs bosons contribute to both loop-induced decay amplitudes $h \rightarrow \gamma\gamma, Z\gamma$ [15]. But in this framework, the recent experimental data of the decay $h \rightarrow \gamma\gamma$ predicts a very small $|\mu_{Z\gamma} - 1| < 4\%$. In Higgs triplet models [16], the situation is the same where it was pointed out that $\text{Br}(h \rightarrow Z\gamma)$ is usually smaller than $\text{Br}(h \rightarrow \gamma\gamma)$. Suppressed values of $|\mu_{Z\gamma} - 1|$ have been shown recently in other Higgs extensions of the SM [17].

In this work, we will focus on another class of the SM extensions, called the 3-3-1 models, which are constructed from the gauge group $SU(2)_C \times SU(3)_L \times U(1)_X$ [18–23]. These models have many interesting features which cannot be explained in the SM framework, for example they can give explanations of the existence of three fermion families, the electric charge quantization [24], the sources of CP violations [25, 26], the strong CP-problem [27–30]. In general, one of the most important parameters to distinguish different 3-3-1 models is denoted as β , which defines electric charges of new particles through the following electric charge operator,

$$Q = T_3 + \beta T_8 + X, \quad (1)$$

where T_3 and T_8 are two diagonal generators of the $SU(3)$ group, X is the $U(1)$ charge. Apart from the popular 3-3-1 models with values of $\beta = \pm\frac{1}{\sqrt{3}}, \pm\sqrt{3}$, other models with $\beta = 0, \pm\frac{2}{\sqrt{3}}, \frac{1}{3\sqrt{3}}$ have been discussed phenomenologically [31–33]. Different phenomenological aspects in models with arbitrary β were also discussed [34–41]. As we will see, the model contains nine electroweak gauge bosons, four of them are identified as the SM-like particles. The remaining include one heavy neutral gauge boson Z' and the two pairs of charged gauge bosons. Popularly, all particles get masses from three Higgs $SU(3)_L$ triplets, including a neutral CP-even Higgs component with a large expectation vacuum value (vev) v_3 that results in heavy masses of the $SU(3)_L$ particles. The three Higgs triplets also contain new charged Higgs bosons that may contribute to the amplitudes of the loop-induced decays of neutral Higgs bosons, including the SM-like one. Correlations among these Higgs and gauge contributions will predict the allowed regions of the parameter space that satisfy the current experimental data of $h \rightarrow \gamma\gamma$. It is interesting to estimate how large of the allowed values of $\mu_{Z\gamma}$ can be.

The decay $h \rightarrow \gamma\gamma$ was mentioned in some particular 3-3-1 models for constraining the parameter space [42, 43]. Both $h \rightarrow \gamma\gamma, Z\gamma$ were also mentioned previously in the 3-3-1

models, but some nontrivial contributions to the amplitude of the decay $h \rightarrow Z\gamma$ were not included [34, 35]. In this work, we will study effects of heavy particles predicted by the 3-3-1 models on the two decays of the SM-like Higgs bosons $h \rightarrow \gamma\gamma, Z\gamma$ and the correlations between two corresponding signal strengths resulting from these effects. We will use more general analytic formulas of one-loop contribution to the decay amplitude $h \rightarrow Z\gamma$ introduced recently [44, 45]. For simplicity in calculating the physical states of the neutral CP-even Higgs bosons, the Higgs potential of the 3-3-1 models will be considered as an effective 2HDM after the first breaking step $SU(3)_L \times U(1)_X \rightarrow SU(2)_L \times U(1)_Y$. This form of the Higgs potential was mentioned in details in ref. [1] for studying a 3-3-1 model with $\beta = -1/\sqrt{3}$. This Higgs potential can be applied to a general 3-3-1 model keeping β as a free parameter, as we will present. This model will be denoted as the 331 β in our work. This can be seen by the fact that two 3-3-1 Higgs triplets have components the same as those appear in the 2HDM. The physical states of neutral Higgs bosons then can be determined exactly at the tree level. The Higgs sector predicted by 2HDMs can be collected, so that the recent theoretical constraint on the Higgs sector of 2HDM [46] can also be included to constrain the parameter space. The property that the 2HDM is contained in the 331 β were concerned previously [39].

On the other hand, the 331 β contains another heavy neutral Higgs boson that does not couple with the SM particle, except the SM-like Higgs boson. Hence, if it is the lightest particle among those beyond the SM, the main decay channels of this particle are the tree level decay in a pair of SM-like Higgs boson and loop-induced decays to pairs of gluons and bosons $\gamma\gamma, Z\gamma$. An investigation to determine which decay channels can be used to distinguish different 3-3-1 models will also be presented.

Our work is arranged as follows. Section II summarizes contents of the 3-3-1 models investigated in this work. All couplings and analytic formulas needed for calculating the Brs and signal strengths of the $h, h_3^0 \rightarrow \gamma\gamma, Z\gamma$ are presented in Section III. Numerical results are shown in Section IV. Important remarks and inclusions are pointed out in Section V. Finally, there are three appendices listing more detailed calculations on couplings, particular analytic formulas for one-loop contributions of different particles to the decay amplitudes of $h, h_3^0 \rightarrow \gamma\gamma, Z\gamma$, and interesting numerical illustrations.

II. 3-3-1 MODEL WITH ARBITRARY β

A. The model review

In this section, we summarize all fermions and Higgs bosons. Left-handed leptons and right-handed leptons are assigned to $SU(3)_L$ anti-triplets and singlets:

$$L'_{aL} = \begin{pmatrix} e'_a \\ -\nu'_a \\ E'_a \end{pmatrix}_L \sim \left(1, 3^*, -\frac{1}{2} + \frac{\beta}{2\sqrt{3}}\right), \quad a = 1, 2, 3,$$

$$e'_{aR} \sim (1, 1, -1), \quad \nu'_{aR} \sim (1, 1, 0), \quad E'_{aR} \sim \left(1, 1, -\frac{1}{2} + \frac{\sqrt{3}\beta}{2}\right), \quad (2)$$

where in the parentheses present the representations and the hypercharge X of the gauge groups $SU(3)_C$, $SU(3)_L$ and $U(1)_X$, respectively. The model includes three right handed (RH) neutrinos ν'_{aR} and heavy exotic leptons $E'_{L,R}$.

The quark sector is arranged to guarantee for anomaly cancellation, namely

$$Q'_{iL} = \begin{pmatrix} u'_i \\ d'_i \\ J'_i \end{pmatrix}_L \sim \left(3, 3, \frac{1}{6} - \frac{\beta}{2\sqrt{3}}\right), \quad Q'_{3L} = \begin{pmatrix} d'_3 \\ -u'_3 \\ J'_3 \end{pmatrix}_L \sim \left(3, 3^*, \frac{1}{6} + \frac{\beta}{2\sqrt{3}}\right), \quad (3)$$

$$u'_{aR} \sim \left(3, 1, \frac{2}{3}\right), \quad d'_{aR} \sim \left(3, 1, \frac{-1}{3}\right),$$

$$J'_{iR} \sim \left(3, 1, \frac{1}{6} - \frac{\sqrt{3}\beta}{2}\right), \quad J'_{3R} \sim \left(3, 1, \frac{1}{6} + \frac{\sqrt{3}\beta}{2}\right), \quad (4)$$

where $i = 1, 2$, $a = 1, 2, 3$, and $J_{aL,R}$ are exotic quarks predicted by the 331β model. There is another arrangement that the model contains three left-handed lepton triplets, one quark triplet and two other quark anti-triplets. But, it was shown that the two arrangements are equivalent in the sense that they predict the same physics [47, 48].

To generate masses for gauge bosons and fermions, three scalar triplets are introduced as follows

$$\chi = \begin{pmatrix} \chi^{+A} \\ \chi^{+B} \\ \chi^0 \end{pmatrix} \sim \left(1, 3, \frac{\beta}{\sqrt{3}}\right), \quad \rho = \begin{pmatrix} \rho^+ \\ \rho^0 \\ \rho^{-B} \end{pmatrix} \sim \left(1, 3, \frac{1}{2} - \frac{\beta}{2\sqrt{3}}\right),$$

$$\eta = \begin{pmatrix} \eta^0 \\ \eta^- \\ \eta^{-A} \end{pmatrix} \sim \left(1, 3, -\frac{1}{2} - \frac{\beta}{2\sqrt{3}}\right), \quad (5)$$

where A, B denote electric charges defined in Eq. (1). These Higgses develop vacuum expectation values (VEV) defined as $\langle \chi^0 \rangle = \frac{v_3}{\sqrt{2}}$, $\langle \rho^0 \rangle = \frac{v_2}{\sqrt{2}}$, $\langle \eta^0 \rangle = \frac{v_1}{\sqrt{2}}$, leading to

$$\chi^0 = \frac{v_3 + r_3 + ia_3}{\sqrt{2}}, \quad \langle \rho^0 \rangle = \frac{v_2 + r_2 + ia_2}{\sqrt{2}}, \quad \langle \eta^0 \rangle = \frac{v_1 + r_1 + ia_1}{\sqrt{2}}. \quad (6)$$

The symmetry breaking happens in two steps: $SU(3)_L \otimes U(1)_X \xrightarrow{v_3} SU(2)_L \otimes U(1)_Y \xrightarrow{v_1, v_2} U(1)_Q$. It is therefore reasonable to assume that $v_3 > v_1, v_2$. At the second breaking step, ρ and η play roles of the two $SU(2)_L$ doublets similar to 2HDM, except differences in coupling with fermions. Masses and physical states of all particles are summarized as follows.

B. Fermions

Masses and physical states of the fermion relating with the Yukawa interactions. The respective Lagrangian for leptons and quark is

$$\mathcal{L}_{\text{lepton}}^Y = -Y_{ab}^e \bar{L}'_{aL} \eta^* e'_{bR} - Y_{ab}^\nu \bar{L}'_{aL} \rho^* \nu'_{bR} - Y_{ab}^E \bar{L}'_{aL} \chi^* E'_{bR} + \text{h.c.}, \quad (7)$$

$$\begin{aligned} \mathcal{L}_{\text{quark}}^Y = & -Y_{ia}^d \bar{Q}'_{iL} \rho d'_{aR} - Y_{3a}^d \bar{Q}'_{3L} \eta^* d'_{aR} - Y_{ia}^u \bar{Q}'_{iL} \eta u_{aR} - Y_{3a}^u \bar{Q}'_{3L} \rho^* u'_{aR} \\ & - Y_{ij}^J \bar{Q}'_{iL} \chi J'_{jR} - Y_{33}^J \bar{Q}'_{3L} \chi^* J'_{3R} + \text{h.c.}, \end{aligned} \quad (8)$$

We note that in some particular values of β , additional terms may appear but a Z_2 symmetry can be imposed to exclude them, see an example given in ref. [1] with the same Yukawa Lagrangian of quarks.

As mentioned above, the SM-like fermions get masses from couplings with two Higgs bosons η and ρ , similarly to the 2HDM. On the other hand, the up (down) quarks couple to both Higgs triplets, leading to a different feature from four popular types of 2HDM, see for example [49], where all up (down) quarks couple to the same Higgs doublet in order to avoid tree level flavor changing neutral currents (FCNCs). As a result, many interesting properties relating with the fermion couplings were pointed out to distinguish 3-3-1 models and 2HDMs [1].

The exotic fermions couple to only χ , implying that only the neutral Higgs component χ^0 couple to these fermions, as we will see below. The neutral Higgs sector in ref. [1] has a

property that the χ^0 does not contribute to the SM-like Higgs boson. As a by product, the SM-like Higgs boson decouples with all exotic fermions, hence they do not contribute to the one-loop decay amplitudes $h \rightarrow \gamma\gamma$ and $h \rightarrow Z\gamma$.

The SM fermion masses are determined based on discussions in refs. [1, 36, 50], where the mixing between quarks are safely ignored in this work. The mass matrices of all fermions are then diagonal. Now, all of the original fermion states are the physical, hence we will denote them by $e_{aL,R}$, $u_{aL,R}$ and $d_{aL,R}$. The fermion masses are given as follows:

$$m_{e_a} = \frac{Y_{aa}^e v_1}{\sqrt{2}}, \quad m_{u_i} = \frac{Y_{ii}^u v_1}{\sqrt{2}}, \quad m_{d_i} = \frac{Y_{ii}^d v_2}{\sqrt{2}}, \quad m_{u_3} = -\frac{Y_{33}^u v_2}{\sqrt{2}}, \quad m_{d_3} = \frac{Y_{33}^d v_1}{\sqrt{2}}, \quad m_{F_a} = \frac{Y_{aa}^F v_3}{\sqrt{2}}, \quad (9)$$

where $Y_{ab}^f = 0 \ \forall a \neq b$, $f = e, u, d, J, E$ and $F = J, E$. The relations (9) will be used to determine Feynman rules of Yukawa couplings in Lagrangians (7) and (8).

C. Gauge bosons

The model contains nine electroweak (EW) gauge bosons corresponding to the 9 generators of the EW gauge group $SU(3)_L \otimes U(1)_X$. The covariant derivative is defined as ¹ [34, 36, 50],

$$D_\mu \equiv \partial_\mu - igT^a W_\mu^a - ig_X X T^9 X_\mu, \quad (10)$$

where $T^9 = 1/\sqrt{6}$, g and g_X are coupling constants of the two groups $SU(3)_L$ and $U(1)_X$, respectively. The matrix $W_\mu^a T^a$, where $T^a = \lambda_a/2$ corresponding to a triplet representation, is

$$W_\mu^a T^a = \frac{1}{2} \begin{pmatrix} W_\mu^3 + \frac{1}{\sqrt{3}} W_\mu^8 & \sqrt{2} W_\mu^+ & \sqrt{2} Y_\mu^{+A} \\ \sqrt{2} W_\mu^- & -W_\mu^3 + \frac{1}{\sqrt{3}} W_\mu^8 & \sqrt{2} V_\mu^{+B} \\ \sqrt{2} Y_\mu^{-A} & \sqrt{2} V_\mu^{-B} & -\frac{2}{\sqrt{3}} W_\mu^8 \end{pmatrix}, \quad (11)$$

where we have defined the mass eigenstates of the charged gauge bosons as

$$W_\mu^\pm = \frac{1}{\sqrt{2}} (W_\mu^1 \mp i W_\mu^2), \quad Y_\mu^{\pm A} = \frac{1}{\sqrt{2}} (W_\mu^4 \mp i W_\mu^5), \quad V_\mu^{\pm B} = \frac{1}{\sqrt{2}} (W_\mu^6 \mp i W_\mu^7), \quad (12)$$

and A, B are electric charges of the corresponding gauge bosons calculated based on Eq. (1),

$$A = \frac{1}{2} + \beta \frac{\sqrt{3}}{2}, \quad B = -\frac{1}{2} + \beta \frac{\sqrt{3}}{2}. \quad (13)$$

¹ This definition is different from Ref. [1] by T^9 .

We note that B is also the electric charge of the new leptons E_a .

The symmetry breaking happens in two steps: $SU(3)_L \otimes U(1)_X \xrightarrow{v_3} SU(2)_L \otimes U(1)_Y \xrightarrow{v_1, v_2} U(1)_Q$, corresponding to the following transformation of the neutral gauge bosons from the original basis to the final physical one: $X_\mu, W_\mu^3, W_\mu^8 \xrightarrow{\theta_{331}} B_\mu, W_\mu^3, Z'_\mu \xrightarrow{\theta_W} A_\mu, Z_\mu, Z'_\mu \xrightarrow{\theta} A_\mu, Z_{1\mu}, Z_{2\mu}$. After the first step, five gauge bosons will be massive and the remaining four massless gauge bosons can be identified with the before-symmetry-breaking SM gauge bosons. The two physical states $Z_{1,2}$ are mixed from the SM and heavy gauge bosons Z_μ and Z'_μ .

It is well-known that

$$g_2 = g, \quad g_1 = g_X \frac{g}{\sqrt{6g^2 + \beta^2 g_X^2}}, \quad (14)$$

where g_2 and g_1 are the two couplings of the SM corresponding to the gauge groups $SU(2)_L$ and $U(1)_Y$, respectively. Using the weak mixing angle defined as $t_W = \tan \theta_W = g_1/g_2$ and we denote $s_W = \sin \theta_W$, it is derived that

$$\frac{g_X^2}{g^2} = \frac{6s_W^2}{1 - (1 + \beta^2)s_W^2} = \frac{6s_W^2}{c_W^2(1 - \beta^2 t_W^2)}, \quad (15)$$

which gives a constraint $|\beta| \leq \sqrt{3}$ used in the numerical analysis.

The masses of the charged gauge bosons are

$$m_Y^2 \equiv m_{Y \pm A}^2 = \frac{g^2}{4}(v_3^2 + v_1^2), \quad m_V^2 \equiv m_{V \pm B}^2 = \frac{g^2}{4}(v_3^2 + v_2^2), \quad m_W^2 \equiv m_{W \pm}^2 = \frac{g^2}{4}(v_1^2 + v_2^2). \quad (16)$$

The matching condition with the SM give $v^2 \equiv v_1^2 + v_2^2 \simeq 246 [\text{GeV}^2]$. Based on Refs. [41, 50], the ratios between VEVs are used to define three mixing parameters as follows

$$s_{ij} \equiv \frac{v_i}{\sqrt{v_i^2 + v_j^2}}, \quad c_{ij} \equiv \sqrt{1 - s_{ij}^2}, \quad t_{ij} \equiv \tan \beta_{ij} = \frac{s_{ij}}{c_{ij}}, \quad (17)$$

where $i < j$ and $i, j = 1, 2, 3$.

The model predicts three neutral gauge bosons including the massless photon. Defining [50]

$$s_{331} \equiv \sin \theta_{331} = \frac{\sqrt{6}g}{\sqrt{6g^2 + \beta^2 g_X^2}} = \sqrt{1 - \beta^2 t_W^2}, \quad c_{331} \equiv \cos \theta_{331} = \beta t_W, \quad (18)$$

the relation between the original and physical base of the neutral gauge bosons are

$$\begin{pmatrix} X_\mu \\ W_\mu^3 \\ W_\mu^8 \end{pmatrix} = \begin{pmatrix} s_{331} & 0 & c_{331} \\ 0 & 1 & 0 \\ c_{331} & 0 & -s_{331} \end{pmatrix} \begin{pmatrix} c_W & -s_W & 0 \\ s_W & c_W & 0 \\ 0 & 0 & 1 \end{pmatrix} \begin{pmatrix} 1 & 0 & 0 \\ 0 & c_\theta & -s_\theta \\ 0 & s_\theta & c_\theta \end{pmatrix} \begin{pmatrix} A_\mu \\ Z_{1\mu} \\ Z_{2\mu} \end{pmatrix} = C \begin{pmatrix} A_\mu \\ Z_{1\mu} \\ Z_{2\mu} \end{pmatrix},$$

$$C = \begin{pmatrix} s_{331}c_W, & (-s_{331}s_Wc_\theta + c_{331}s_\theta), & (s_{331}s_Ws_\theta + c_{331}c_\theta) \\ s_W, & c_Wc_\theta, & -s_\theta c_w \\ c_{331}c_W, & -(c_{331}s_Wc_\theta + s_{331}s_\theta), & (c_{331}s_Ws_\theta - s_{331}c_\theta) \end{pmatrix}, \quad (19)$$

where in the limit $v^2 \ll v_3^2$, the mixing angle θ is determined as [41]

$$s_\theta \equiv \sin \theta = \left(3\beta \frac{s_W^2}{c_W^2} + \frac{\sqrt{3}(t_{21}^2 - 1)}{t_{21}^2 + 1} \right) \frac{\sqrt{1 - \beta^2 t_W^2} v^2}{4c_W v_3^3}, \quad (20)$$

and $M_{Z'}^2 = g^2 v_3^2 / (3s_{331}^2) + \mathcal{O}(v^2)$.

To continue, the neutral gauge bosons will be identified as $Z_1 \equiv Z$ and $Z_2 \equiv Z'$, where Z is the one found experimentally.

D. Higgs bosons

The scalar potential is

$$\begin{aligned} V_h = & \mu_1^2 \eta^\dagger \eta + \mu_2^2 \rho^\dagger \rho + \mu_3^2 \chi^\dagger \chi + \lambda_1 (\eta^\dagger \eta)^2 + \lambda_2 (\rho^\dagger \rho)^2 + \lambda_3 (\chi^\dagger \chi)^2 \\ & + \lambda_{12} (\eta^\dagger \eta) (\rho^\dagger \rho) + \lambda_{13} (\eta^\dagger \eta) (\chi^\dagger \chi) + \lambda_{23} (\rho^\dagger \rho) (\chi^\dagger \chi) \\ & + \tilde{\lambda}_{12} (\eta^\dagger \rho) (\rho^\dagger \eta) + \tilde{\lambda}_{13} (\eta^\dagger \chi) (\chi^\dagger \eta) + \tilde{\lambda}_{23} (\rho^\dagger \chi) (\chi^\dagger \rho) - \sqrt{2} f (\epsilon_{ijk} \eta^i \rho^j \chi^k + \text{h.c.}) . \end{aligned} \quad (21)$$

The minimum conditions of the Higgs potential can be found easily [36, 50]. After that, we can take μ_i^2 as functions of other independent parameters then insert them into the Higgs potential (21) to determine the masses and physical states of all Higgs bosons.

The relations between original and mass eigenstates of charged Higgs bosons are [36, 50]:

$$\begin{pmatrix} \phi_W^\pm \\ H^\pm \end{pmatrix} = R(\beta_{12}) \begin{pmatrix} \rho^\pm \\ \eta^\pm \end{pmatrix}, \quad m_{\phi_W} = 0, \quad m_{H^\pm}^2 = \frac{\tilde{\lambda}_{12} v^2}{2} + \frac{f v_3}{2s_{12}c_{12}}, \quad (22)$$

$$\begin{pmatrix} \phi_Y^{\pm A} \\ H^{\pm A} \end{pmatrix} = R(\beta_{13}) \begin{pmatrix} \chi^{\pm A} \\ \eta^{\pm A} \end{pmatrix}, \quad m_{\phi_Y} = 0, \quad m_{H^{\pm A}}^2 = \left(\frac{\tilde{\lambda}_{13}}{2} + \frac{f}{t_{12}v_3} \right) (v_1^2 + v_3^2), \quad (23)$$

$$\begin{pmatrix} \phi_V^{\pm B} \\ H^{\pm B} \end{pmatrix} = R(\beta_{23}) \begin{pmatrix} \chi^{\pm B} \\ \rho^{\pm B} \end{pmatrix}, \quad m_{\phi_V} = 0, \quad m_{H^{\pm B}}^2 = \left(\frac{\tilde{\lambda}_{23}}{2} + \frac{t_{12}f}{v_3} \right) (v_2^2 + v_3^2), \quad (24)$$

where we have define a rotation $R(x)$ as

$$R(x) \equiv \begin{pmatrix} c_x & -s_x \\ s_x & c_x \end{pmatrix}. \quad (25)$$

The massless states ϕ_W^\pm , $\phi_Y^{\pm A}$, and $\phi_V^{\pm B}$ are goldstone bosons absorbed by the physical gauge bosons.

For neutral Higgs bosons, to avoid the tree level contribution of SM-like Higgs bosons to the flavor changing neutral currents (FCNC) in the quark sector, we follow the aligned limit introduced in Ref. [1], namely

$$f = \lambda_{13} t_{12} v_3 = \frac{\lambda_{23} v_3}{t_{12}}. \quad (26)$$

As a result, we will choose f and λ_{23} as functions of the remaining. This leads to the following form of the CP-even neutral squared mass matrix corresponding to the basis (r_1, r_2, r_3) :

$$M_r^2 = \begin{pmatrix} 2\lambda_1 s_{12}^2 v^2 + \lambda_{13} v_3^2 & t_{12} (\lambda_{12} c_{12}^2 v^2 - \lambda_{13} v_3^2) & 0 \\ t_{12} (\lambda_{12} c_{12}^2 v^2 - \lambda_{13} v_3^2) & 2c_{12}^2 \lambda_2 v^2 + t_{12}^2 \lambda_{13} v_3^2 & 0 \\ 0 & 0 & s_{12}^2 \lambda_{13} v^2 + 2\lambda_3 v_3^2 \end{pmatrix}. \quad (27)$$

As a result, $r_3 \equiv h_3^0$ is a physical CP-even neutral Higgs boson with mass $m_{h_3^0}^2 = \lambda_{13} s_{12}^2 v^2 + 2\lambda_3 v_3^2$. The sub-matrix 2×2 in Eq. (27) is denoted as $M_r'^2$, which is diagonalized as follows [1],

$$R(\alpha) M_r'^2 R^T(\alpha) = \text{diag}(m_{h_1^0}^2, m_{h_2^0}^2), \quad (28)$$

where

$$\alpha \equiv \beta_{12} - \frac{\pi}{2} + \delta, \quad (29)$$

$$\tan 2\delta = \frac{2M_{12}^2}{M_{22}^2 - M_{11}^2} \sim \mathcal{O}\left(\frac{v^2}{v_3^2}\right), \quad (30)$$

$$m_{h_1^0}^2 = M_{11}^2 \cos^2 \delta + M_{22}^2 \sin^2 \delta - M_{12}^2 \sin 2\delta, \quad (31)$$

$$m_{h_2^0}^2 = M_{11}^2 \sin^2 \delta + M_{22}^2 \cos^2 \delta + M_{12}^2 \sin 2\delta, \quad (32)$$

$$M_{11}^2 = 2 (s_{12}^4 \lambda_1 + c_{12}^4 \lambda_2 + s_{12}^2 c_{12}^2 \lambda_{12}) v^2 = \mathcal{O}(v^2),$$

$$M_{12}^2 = [-\lambda_1 s_{12}^2 + \lambda_2 c_{12}^2 + \lambda_{12} (s_{12}^2 - c_{12}^2)] s_{12} c_{12} v^2 = \mathcal{O}(v^2),$$

$$M_{22}^2 = 2s_{12}^2 c_{12}^2 [\lambda_1 + \lambda_2 - \lambda_{12}] v^2 + \frac{\lambda_{13} v_3^2}{c_{12}^2}.$$

We also have

$$\begin{pmatrix} r_1 \\ r_2 \end{pmatrix} = R^T(\alpha) \begin{pmatrix} h_1^0 \\ h_2^0 \end{pmatrix}. \quad (33)$$

To determine the SM-like Higgs boson, we firstly look at the Eq. (30), which give $\delta = \mathcal{O}(\frac{v^2}{v_3^2}) \simeq 0$ when $v^2 \ll v_3^2$. In this limit, $m_h^2 = M_{11}^2 + v^2 \times \mathcal{O}(\frac{v^2}{v_3^2}) \sim M_{11}^2$ while $m_{h_2^0}^2 =$

$M_{22}^2 + v^2 \times \mathcal{O}(\frac{v^2}{v_3^2}) \simeq M_{22}^2$. Hence, $h_1^0 \equiv h$ is identified with the SM-like Higgs boson found at LHC. Furthermore, in the following calculation we will see more explicitly that the couplings of this Higgs boson are the same as those given in the SM in the limit $\delta \rightarrow 0$.

From the constant trace of the squared mass matrix, the λ_{13} can be written as

$$\lambda_{13} = \frac{c_{12}^2}{v_3^2} \left[m_{h_1^0}^2 + m_{h_2^0}^2 - 2v^2 (s_{12}^2 \lambda_1 + c_{12}^2 \lambda_2) \right]. \quad (34)$$

We will choose δ , $m_{h_1^0}$ and $m_{h_2^0}$ as input parameters. The λ_{13} , λ_{12} and λ_2 are dependent parameters, namely

$$\begin{aligned} \lambda_2 &= t_{12}^4 \lambda_1 + \frac{-[c_\delta^2(t_{12}^2 - 1) + t_{12}s_{2\delta}]m_{h_1^0}^2 + [s_\delta^2(1 - t_{12}^2) + s_{2\delta}t_{12}]m_{h_2^0}^2}{2c_{12}^2 v^2}, \\ \lambda_{12} &= -2t_{12}^2 \lambda_1 + \frac{(s_{2\delta} + 2t_{12}c_\delta^2)m_{h_1^0}^2 + (-s_{2\delta} + 2t_{12}s_\delta^2)m_{h_2^0}^2}{2s_{12}c_{12}v^2}, \end{aligned} \quad (35)$$

and λ_{13} was given in Eq. (34).

The Higgs self couplings should satisfy all constraints discussed recently to guarantee the vacuum stability of the Higgs potential [51], the perturbative limits, and the positive squared masses of all Higgs bosons. We note that in the case of absence the relations in Eq. (26), the mixing between SM-like Higgs bosons with other heavy neutral Higgs still suppressed due to large $v_3 > 5$ TeV enough to cancel the FCNCs in 3-3-1 models [52].

III. COUPLINGS AND ANALYTIC FORMULAS INVOLVED WITH LOOP-INDUCED HIGGS DECAYS

A. Couplings

From the above discussion on the Higgs potential, we can derive all Higgs self-couplings of the SM-like Higgs boson relating to the decays $h \rightarrow Z\gamma$ and $h \rightarrow \gamma\gamma$, using the interacting Lagrangian $\mathcal{L}_{hHH} = -V_h$. The Feynman rules are given in Table I, where each factor $-i\lambda_{hss}$ corresponds to a vertex hss , where $s = H^\pm, H^{\pm A}, H^{\pm B}$.

Based on the Yukawa Lagrangians (7) and (8), the couplings of the SM-like Higgs boson with SM fermions can be determined, see also in table I, where we have used the relation (29). The notation of the Feynman rule is $-i(Y_{h\bar{f}fL}P_L + Y_{h\bar{f}fR}P_R)$ for each vertex $h\bar{f}f$. For SM lepton in this case, we always have $Y_{\bar{f}fL} = Y_{\bar{f}fR}$, which are given in table II. Both neutral

Vertex	Coupling: $-i\lambda_{hss}$
$-i\lambda_{hH^+H^-}$	$iv \left[2s_{12}c_{12} (-\lambda_1c_{12}c_\alpha + \lambda_2s_{12}s_\alpha) + (s_\alpha c_{12}^3 - c_\alpha s_{12}^3) \lambda_{12} - c_\delta \tilde{\lambda}_{12} \right]$
$-i\lambda_{hH^AH^-A}$	$ic_{13}^2 \left\{ v \left[s_\alpha c_{12} (\lambda_{12} + t_{13}^2 \lambda_{23}) - c_\alpha s_{12} (2\lambda_1 + t_{13}^2 (\lambda_{13} + \tilde{\lambda}_{13})) \right] + v_3 t_{13} \left(\frac{2fs_\alpha}{v_3} - c_\alpha \tilde{\lambda}_{13} \right) \right\}$
$-i\lambda_{hH^BH^-B}$	$ic_{23}^2 \left\{ v \left[s_\alpha c_{12} (2\lambda_2 + t_{23}^2 (\lambda_{23} + \tilde{\lambda}_{23})) - c_\alpha s_{12} (\lambda_{12} + t_{23}^2 \lambda_{13}) \right] + v_3 t_{23} \left(s_\alpha \tilde{\lambda}_{23} - \frac{2fc_\alpha}{v_3} \right) \right\}$

TABLE I: Feynman rules for the SM-like Higgs boson couplings with charged Higgs bosons

$-iY_{h\bar{e}_a e_a L,R}$	$-iY_{h\bar{u}_i u_i L,R}$	$-iY_{h\bar{u}_3 u_3 L,R}$	$-iY_{h\bar{d}_i d_i L,R}$	$-iY_{h\bar{d}_3 d_3 L,R}$
$-i\frac{m_{e_a}}{v} \left(c_\delta - \frac{s_\delta}{t_{12}} \right)$	$-i\frac{m_{u_i}}{v} \left(c_\delta - \frac{s_\delta}{t_{12}} \right)$	$-i\frac{m_{u_3}}{v} (c_\delta + t_{12}s_\delta)$	$-i\frac{m_{d_i}}{v} (c_\delta + t_{12}s_\delta)$	$-i\frac{m_{d_3}}{v} \left(c_\delta - \frac{s_\delta}{t_{12}} \right)$

TABLE II: Yukawa couplings of the SM-like Higgs boson

CP-even Higgs bosons h and h_2^0 do not couple to exotic fermion in the aligned limit (26). In contrast, h_3^0 couple only to the exotic fermions, while do not couple with the SM ones.

The couplings of Higgs and gauge bosons are contained in the covariant kinetic terms of the Higgs bosons

$$\begin{aligned}
\mathcal{L}_{\text{kin}}^H &= (D_\mu \chi)^\dagger (D^\mu \chi) + (D_\mu \rho)^\dagger (D^\mu \rho) + (D_\mu \eta)^\dagger (D^\mu \eta) \\
&\rightarrow g_{hvv} g_{\mu\nu} h v^{-Q_\mu} v^{Q_\nu}, \\
&\quad -ig_{hsv}^* v^{-Q_\mu} (s^{+Q} \partial_\mu h - h \partial_\mu s^{+Q}), ig_{hsv} v^{Q_\mu} (s^{-Q} \partial_\mu h - h \partial_\mu s^{-Q}), \\
&\quad ig_{Zss} Z^\mu (s^{-Q} \partial_\mu s^Q - s^Q \partial_\mu s^{-Q}), ig_{Zvs} Z^\mu v^{Q_\nu} s^{-Q} g_{\mu\nu}, ig_{Zvs}^* Z^\mu v^{-Q_\nu} s^Q g_{\mu\nu}, \\
&\quad ieQA^\mu (s^{-Q} \partial_\mu s^Q - s^Q \partial_\mu s^{-Q}), \tag{36}
\end{aligned}$$

where $s = H^\pm, H^{\pm A}, H^{\pm B}$. From the second line we list the relevant terms contributing to the decays $h \rightarrow Z\gamma, \gamma\gamma$. The corresponding Feynman rules are shown in Table III, where $\partial_\mu h \rightarrow -ip_0 \mu h$ and $\partial_\mu s^{\pm Q} \rightarrow -ip_\pm \mu s^{\pm Q}$ and the relation (29) was used. The notations p_0, p_\pm are incoming momenta.

Vertex	Coupling:	Vertex	Coupling
$g_{hW^+W^-}$	$g m_W c_\delta$	$g_{hY^+AY^-A}$	$g m_W c_\alpha s_{12}$
$g_{hV^+BV^-B}$	$-g m_W s_\alpha c_{12}$	$g_{hH^-W^+}$	$\frac{g s_\delta}{2}$
$g_{hH^-AY^A}$	$-\frac{g c_{13} c_\alpha}{2}$	$g_{hH^-BV^B}$	$\frac{g c_{23} s_\alpha}{2}$

TABLE III: Feynman rules for couplings of the SM-like Higgs boson to Higgs and gauge bosons.

The Feynman rules of couplings of Z to charged Higgs and gauge boson in (36) are given

in table IV.

Vertex	Coupling
$g_{ZH^+H^-}$	$\frac{g}{2c_W} \left(c_\theta c_{2W} + \frac{s_\theta [\sqrt{3}c_W^2(1-2s_{12}^2)+3\beta s_W^2]}{3c_W\sqrt{1-\beta^2 t_W^2}} \right)$
$g_{ZH^A H^{-A}}$	$\frac{g}{2c_W} \left(c_\theta [s_{13}^2 - (1 + \sqrt{3}\beta)s_W^2] + \frac{s_\theta [\sqrt{3}c_W^2(s_{13}^2-2)+3\beta(\sqrt{3}\beta+c_{13}^2)s_W^2]}{3c_W\sqrt{1-\beta^2 t_W^2}} \right)$
$g_{ZH^B H^{-B}}$	$\frac{ig}{2c_W} \left(-c_\theta [s_{23}^2 + (\sqrt{3}\beta - 1)s_W^2] + \frac{s_\theta [\sqrt{3}c_W^2(s_{23}^2-2)+3\beta(\sqrt{3}\beta-c_{23}^2)s_W^2]}{3c_W\sqrt{1-\beta^2 t_W^2}} \right)$
$g_{ZW^+H^-}$	$-\frac{g m_W(2s_{12}c_{12}s_\theta)}{\sqrt{3(1-\beta^2 t_W^2)}}$
$g_{ZY^A H^{-A}},$ $g_{ZY^{-A} H^A}$	$\frac{g^2 c_{13}}{4} \left\{ c_\theta c_W [s_{12} (1 + (2 + \sqrt{3}\beta)t_W^2) v + t_{13}(1 - \sqrt{3}\beta t_W^2)v_3] \right.$ $\left. + \frac{s_\theta}{3\sqrt{1-\beta^2 t_W^2}} [s_{12} (\sqrt{3} - 3\beta(2 + \sqrt{3}\beta)t_W^2) v + \sqrt{3}t_{13} (1 + 3\beta^2 t_W^2) v_3] \right\}$
$g_{ZV^B H^{-B}},$ $g_{ZV^{-B} H^B}$	$\frac{g^2 c_{23}}{4} \left\{ c_\theta c_W [c_{12} (-1 + (-2 + \sqrt{3}\beta)t_W^2) v - t_{23}(1 + \sqrt{3}\beta t_W^2)v_3] \right.$ $\left. + \frac{s_\theta}{3\sqrt{1-\beta^2 t_W^2}} [c_{12} (\sqrt{3} - 3\beta(-2 + \sqrt{3}\beta)t_W^2) v + \sqrt{3}t_{23} (1 + 3\beta^2 t_W^2) v_3] \right\}$

TABLE IV: Feynman rules of couplings with Z and photon. Notations p_+ and p_- are incoming momenta.

The couplings of Z and photon A_μ with fermions arise from the covariant kinetic of fermion:

$$\begin{aligned}
\mathcal{L}_{\text{kin}}^f &= \sum_{a=1}^3 (\overline{L_{aL}} \gamma^\mu D_\mu L_{aL} + \overline{\nu_{aR}} \gamma^\mu \partial_\mu \nu_{aR} + \overline{e_{aR}} \gamma^\mu D_\mu e_{aR} + \overline{E_{aR}} \gamma^\mu D_\mu E_{aR}) \\
&+ \sum_{a=1}^3 (\overline{Q_{aL}} \gamma^\mu D_\mu Q_{aL} + \overline{u_{aR}} \gamma^\mu D_\mu u_{aR} + \overline{d_{aR}} \gamma^\mu D_\mu d_{aR} + \overline{J_{aR}} \gamma^\mu D_\mu J_{aR}) \\
&\supset \sum_f \left[\frac{g c_\theta}{c_W} \bar{f} \gamma^\mu (g_L^f P_L + g_R^f P_R) f Z_\mu + e Q_f \bar{f} \gamma^\mu f A_\mu \right], \tag{37}
\end{aligned}$$

where f runs over all fermions in the 3-3-1 β model, Q_f is the electric charge of the f . Values of $g_{L,R}^f$ are shown in table V.

The couplings of three gauge bosons arise from the covariant kinetic Lagrangian of the non-Abelian gauge bosons:

$$\mathcal{L}_D^g = -\frac{1}{4} \sum_{a=1}^8 F_{\mu\nu}^a F^{a\mu\nu}, \tag{38}$$

where

$$F_{\mu\nu}^a = \partial_\mu W_\nu^a - \partial_\nu W_\mu^a + g \sum_{b,c=1}^8 f^{abc} W_\mu^b W_\nu^c, \tag{39}$$

f	g_L^f	g_R^f
e_a	$-\frac{1}{2} + s_W^2 + \frac{t_\theta c_W (1 - \sqrt{3}\beta t_W^2)}{2\sqrt{3(1 - \beta^2 t_W^2)}}$	$s_W^2 \left(1 - \frac{t_\theta \beta}{c_W \sqrt{1 - \beta^2 t_W^2}} \right)$
u_i	$\frac{1}{2} - \frac{2}{3}s_W^2 + \frac{t_\theta c_W (\beta t_W^2 - \sqrt{3})}{6\sqrt{1 - \beta^2 t_W^2}}$	$-\frac{2}{3}s_W^2 \left(1 - \frac{t_\theta \beta}{c_W \sqrt{1 - \beta^2 t_W^2}} \right)$
u_3	$\frac{1}{2} - \frac{2}{3}s_W^2 + \frac{t_\theta c_W (\beta t_W^2 + \sqrt{3})}{6\sqrt{1 - \beta^2 t_W^2}}$	$-\frac{2}{3}s_W^2 \left(1 - \frac{t_\theta \beta}{c_W \sqrt{1 - \beta^2 t_W^2}} \right)$
d_i	$-\frac{1}{2} + \frac{1}{3}s_W^2 + \frac{t_\theta c_W (\beta t_W^2 - \sqrt{3})}{6\sqrt{1 - \beta^2 t_W^2}}$	$\frac{1}{3}s_W^2 \left(1 - \frac{t_\theta \beta}{c_W \sqrt{1 - \beta^2 t_W^2}} \right)$
d_3	$-\frac{1}{2} + \frac{1}{3}s_W^2 + \frac{t_\theta c_W (\beta t_W^2 + \sqrt{3})}{6\sqrt{1 - \beta^2 t_W^2}}$	$\frac{1}{3}s_W^2 \left(1 - \frac{t_\theta \beta}{c_W \sqrt{1 - \beta^2 t_W^2}} \right)$

TABLE V: Couplings of Z with fermions

f^{abc} ($a, b, c = 1, 2, \dots, 8$) are structure constants of the $SU(3)$ group. They are defined as

$$\begin{aligned} \mathcal{L}_D^g \rightarrow & -g_{Zvv} Z^\mu(p_0) v^{+Q\nu}(p_+) v^{-Q\lambda}(p_-) \times \Gamma_{\mu\nu\lambda}(p_0, p_+, p_-), \\ & -eQA^\mu(p_0) v^{+Q\nu}(p_+) v^{-Q\lambda}(p_-) \times \Gamma_{\mu\nu\lambda}(p_0, p_+, p_-), \end{aligned} \quad (40)$$

where $\Gamma_{\mu\nu\lambda}(p_0, p_+, p_-) \equiv g_{\mu\nu}(p_0 - p_+)_\lambda + g_{\nu\lambda}(p_+ - p_-)_\mu + g_{\lambda\mu}(p_- - p_0)_\lambda$, and $v = W, V, Y$.

We pay attention on the quartic couplings of the Z and photon with charged gauge bosons.

The involving couplings of Z are given in table VI. These triple couplings were also given in

Vertex	Coupling
$-ig_{ZW+\nu W-\lambda}$	$-igc_W c_\theta$
$-ig_{ZY^A Y-A}$	$\frac{ig}{2} \left[c_\theta (-c_W + \sqrt{3}\beta s_W t_W) + s_\theta \sqrt{3 - 3\beta^2 t_W^2} \right]$
$-ig_{ZV^B Y-B}$	$\frac{ig}{2} \left[c_\theta (c_W + \sqrt{3}\beta s_W t_W) + s_\theta \sqrt{3 - 3\beta^2 t_W^2} \right]$

TABLE VI: Feynman rules for triple gauge couplings relating with the decay $h \rightarrow Z\gamma, \gamma\gamma$.

ref. [34, 53] in the limit $\theta = 0$.

B. Partial decay widths and signal strengths of the SM-like Higgs decays $h \rightarrow Z\gamma, \gamma\gamma$

In the unitary gauge, the above couplings generate one-loop three point Feynman diagrams to the decay amplitude of the SM-like Higgs boson $h \rightarrow Z\gamma$ given in Fig. 1.

The partial decay width is [44, 54]

$$\Gamma(h \rightarrow Z\gamma) = \frac{m_h^3}{32\pi} \times \left(1 - \frac{m_Z^2}{m_h^2} \right)^3 |F_{21}|^2, \quad (41)$$

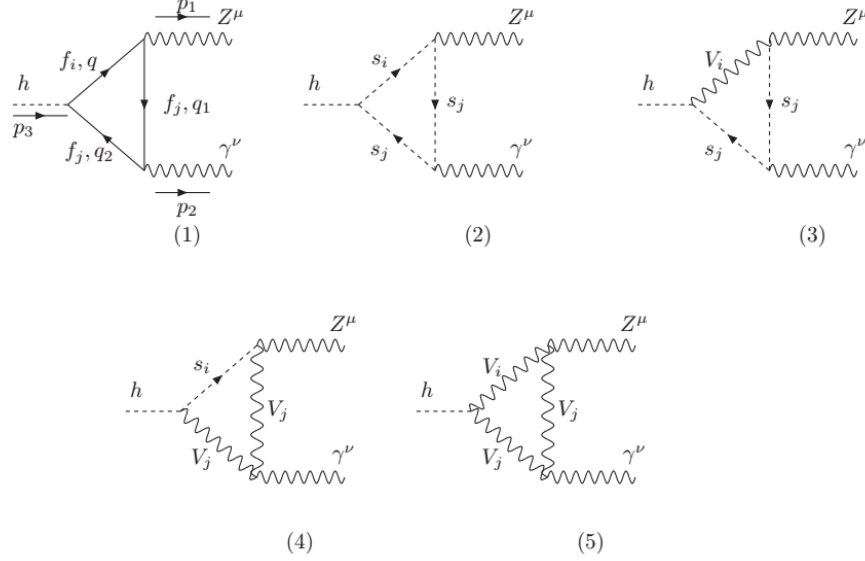


FIG. 1: One-loop three-point Feynman diagrams contributing to the decay $h \rightarrow Z\gamma$ in the unitary gauge, where $f_{i,j}$ are the SM leptons, $s_{i,j} = H^\pm, H^{\pm A}, H^{\pm B}$, $v_{i,j} = W^\pm, Y^{\pm A}, V^{\pm B}$.

where the scalar factors F_{21} and F_5 were mentioned previously for specific one-loop diagrams [44, 54]. More general formulas were given in Ref. [45], leading the following expression

$$F_{21}^{331} = \sum_f F_{21,f}^{331} + \sum_s F_{21,s}^{331} + \sum_v F_{21,v}^{331} + \sum_{\{s,v\}} (F_{21,vs}^{331} + F_{21,sv}^{331}). \quad (42)$$

We note that $F_{21,vs}^{331}$ and $F_{21,sv}^{331}$ were not included in previous works [34, 35].

The detailed analytic formulas of particular expressions are given in appendix B. The partial decay width of the decay $h \rightarrow \gamma\gamma$ can be calculated as [44, 45]

$$\Gamma(h \rightarrow \gamma\gamma) = \frac{m_h^3}{64\pi} \times |F_{\gamma\gamma}^{331}|^2, \quad (43)$$

where

$$F_{\gamma\gamma}^{331} = \sum_f F_{\gamma\gamma,f}^{331} + \sum_s F_{\gamma\gamma,s}^{331} + \sum_v F_{\gamma\gamma,v}^{331}. \quad (44)$$

The detailed analytic formulas of particular expressions are given in appendix B.

To determine the Br of a SM-like Higgs decay, we need to know the total decay width. In the SM, this quantity is sum of the five channels, namely [5, 6]

$$\Gamma_h^{\text{SM}} = \sum_{q \neq t} \Gamma^{\text{SM}}(h \rightarrow \bar{q}q) + \sum_{\ell=e,\mu,\tau} \Gamma^{\text{SM}}(h \rightarrow \ell^+ \ell^-) + \Gamma^{\text{SM}}(h \rightarrow WW^*) + \Gamma^{\text{SM}}(h \rightarrow ZZ^*)$$

$$+ \Gamma^{\text{SM}}(h \rightarrow \gamma\gamma) + \Gamma^{\text{SM}}(h \rightarrow Z\gamma) + \Gamma^{\text{SM}}(h \rightarrow gg), \quad (45)$$

where the particular values of partial decay widths are well-known with Higgs boson mass of 125.09 GeV found experimentally [55]. The Br of a particular decay channel $h \rightarrow X$, where $X = gg, \gamma\gamma, Z\gamma$, is:

$$\text{Br}^{\text{SM}}(h \rightarrow X) \equiv \frac{\Gamma^{\text{SM}}(h \rightarrow X)}{\Gamma_h^{\text{SM}}}. \quad (46)$$

The numerical values are given in table VII [5, 6], where the diphoton decay is consistent with that used in ref. [4], $\text{Br}(h \rightarrow \gamma\gamma) = (2.27 \pm 0.07) \times 10^{-3}$. The recent global signal

$b\bar{b}$	$\tau^+\tau^-$	$\mu^+\mu^-$	$c\bar{c}$	gg	$\gamma\gamma$	$Z\gamma$	WW	ZZ	$\Gamma_h^{\text{SM}} \text{ (GeV)}$
0.5809	0.06256	2.171×10^{-4}	0.02884	0.0818	0.00227	0.001541	0.2152	0.02641	4.10×10^{-3}

TABLE VII: Branching ratios of the SM Higgs boson decays with mass of 125.09 GeV.

strength found experimentally by ATLAS is $\mu_{\gamma\gamma} = 0.99 \pm 0.14$ [4]².

The total decay width of the SM-like Higgs boson predicted by the 331 β is computed based on the deviations of Higgs coupling with fermions and gauge bosons between the two models SM and 331 β , as given in tables I and III. The result is

$$\begin{aligned} \Gamma_h^{331} &= 0.6725 \left(c_\delta - \frac{s_\delta}{t_{12}} \right)^2 \Gamma_h^{\text{SM}} \\ &+ c_\delta^2 \left[0.2152 + \left(1 - \frac{2c_\theta s_\theta c_W}{\sqrt{1 - \beta^2 t_W^2}} \left(\beta t_W^2 + \frac{s_{12}c_\alpha + c_{12}s_\alpha}{\sqrt{3}c_\delta} \right) \right)^2 0.02641 \right] \Gamma_h^{\text{SM}} \\ &+ \Gamma^{331}(h \rightarrow \gamma\gamma) + \Gamma^{331}(h \rightarrow Z\gamma) + \Gamma^{331}(h \rightarrow gg). \end{aligned} \quad (47)$$

There are three loop-induced decays $h \rightarrow \gamma\gamma, Z\gamma, gg$. The SM-like Higgs boson does not couple with the exotic quarks in the 331 β , we can consider only the top quark contribution to the loop contributing to the decay $h \rightarrow gg$. This results in

$$\Gamma^{331}(h \rightarrow gg) = (c_\delta + t_{12}s_\delta)^2 \Gamma^{\text{SM}}(h \rightarrow gg), \quad (48)$$

where the deviation comes from the $ht\bar{t}$ coupling listed in table I. This is consistent with recent investigation for $h \rightarrow \gamma\gamma$ in a 3-3-1 model [43].

² This value gives the same numerical discussion with that reported in [86, 87].

The branching ratio of a SM-like Higgs boson decay $h \rightarrow X$ with $X = \gamma\gamma, Z\gamma$ is

$$\text{Br}^{331}(h \rightarrow X) \equiv \frac{\Gamma^{331}(h \rightarrow X)}{\Gamma_h^{331}}. \quad (49)$$

Many experimental measurements for the SM-like Higgs boson were reported in ref. [56].

We also consider the SM-like Higgs production through the gluon fusion process ggF at LHC. The respective signal strength predicted by 331β is defined as:

$$\mu_{ggF}^{331} \equiv \frac{\sigma^{331}(gg \rightarrow h)}{\sigma^{\text{SM}}(gg \rightarrow h)} \simeq (c_\delta + t_{12}s_\delta)^2, \quad (50)$$

where the last value comes from our assumption that only the main contribution from top quark in the loop is considered. The signal strength of an individual decay channel is

$$\mu_X^{331} \equiv (c_\delta + t_{12}s_\delta)^2 \times \frac{\text{Br}^{331}(h \rightarrow X)}{\text{Br}^{\text{SM}}(h \rightarrow X)}. \quad (51)$$

The recent signal strengths of the two loop-induced decays are $\mu_{\gamma\gamma} = 0.99 \pm 0.14$ [4] and $\mu_{Z\gamma} < 6.6(5.2)$ [7, 55].

C. Decays of the neutral Higgs boson h_3^0

In the above discussion we derive only couplings that contribute to the one-loop amplitudes of the two SM-like Higgs decay channels $h \rightarrow \gamma\gamma, Z\gamma$. Other interesting couplings are listed in the appendix A. Here we stress a very interesting property of the heavy neutral Higgs boson h_3^0 that it has only one non-zero coupling with two SM particles, namely only $\lambda_{h_2 h_3^0} \neq 0$ hence, if $m_{h_3^0} < 2m_{h_1^0}$, it may be stable, consequently may be a DM candidate. But, we should pay attention to the loop-induced decays such as $h_3^0 \rightarrow \gamma\gamma, gg, Z\gamma$ which will be calculated in details below. In addition, if $m_{h_3^0} < m_h/2$ the decay $h \rightarrow h_3^0 h_3^0$ will appear and it should satisfy the invisible decay constraint of SM-like Higgs boson, like a recent study on the inert two Higgs doublet model [57]. In contrast, if $m_{h_3^0} > 2m_h$ and if it is lighter than all other exotic particles predicted by the 331β model, only the tree level decay $h_3^0 \rightarrow hh$ appears, then its total decay width must satisfy the condition $\Gamma_{h_3^0} < 1.3 \times 2\pi \times 10^{-42}$ GeV [58–60]. Unfortunately, there still exist loop-induced decays such as $h_3^0 \rightarrow gg, \gamma\gamma, Z\gamma$ which predict large total decay width of the h_3^0 , as we will show below. Hence h_3^0 can not be a dark matter candidate. Anyway, DM candidates as scalar 3-3-1 Higgs bosons were pointed out previously [61–63].

The couplings of neutral heavy Higgs bosons $h_{2,3}^0$ to fermions are

$$Y_{h_2^0 ffL,R} = \begin{cases} \frac{m_f}{v} \left(\frac{c_\delta}{t_{12}} + s_\delta \right), & f = e_a, u_i, d_3 \\ \frac{m_f}{v} (-c_\delta t_{12} + s_\delta), & f = u_3, d_i \\ 0, & f = E_a, J_a. \end{cases}, \quad Y_{h_3^0 ffL,R} = \begin{cases} 0 & f = e_a, u_a, d_a \\ \frac{m_f}{v_3} & f = E_a, J_a \end{cases}. \quad (52)$$

One interesting point is that h_3^0 couple to only exotic fermions, similar to the heavy neutral Higgs appeared in a $SU(2)_1 \times SU(2)_2 \times U(1)_Y$ model [64], where the partial decay width $h_3^0 \rightarrow gg$ is [54, 65],

$$\Gamma(h_3^0 \rightarrow gg) \simeq \frac{\alpha_s^2 m_{h_3^0}^3}{32\pi^3 v_3^2} \left| \sum_{a=1}^3 t_a [1 + (1 - t_a)f(t_a)] \right|^2, \quad (53)$$

where $t_a \equiv 4m_{J_a}^2/m_{h_3^0}^2$,

$$f(x) = \begin{cases} \arcsin^2 \frac{1}{\sqrt{x}}, & x \geq 1 \\ -\frac{1}{4} \left[\ln \frac{1+\sqrt{1-x}}{1-\sqrt{1-x}} - i\pi \right]^2, & x < 1. \end{cases} \quad (54)$$

In the limit $t_a \gg 1 \forall a = 1, 2, 3$, Eq. (53) can be estimated as [64]

$$\Gamma(h_3^0 \rightarrow gg) \simeq \frac{\alpha_s^2 m_{h_3^0}^3}{8\pi^3 v_3^2}. \quad (55)$$

Furthermore, the production cross-section of this Higgs boson through the gluon-gluon fusion can be estimated from the two gluon decay channel [64].

The partial width of the tree level decay $h_3^0 \rightarrow hh$ when $m_{h_3^0} > 2m_h$ is [1]

$$\Gamma(h_3^0 \rightarrow hh) = \frac{|\lambda_{h_3^0 hh}|^2}{8\pi m_{h_3^0}} \sqrt{1 - \frac{4m_h^2}{m_{h_3^0}^2}} = \frac{\lambda_{13}^2 s_\delta^4 v_3^2}{8\pi c_{12}^4 m_{h_3^0}} \sqrt{1 - \frac{4m_h^2}{m_{h_3^0}^2}}, \quad (56)$$

where λ_{13} was given in Eq. (34).

The total decay width of the h_3^0 is then

$$\Gamma_{h_3^0} = \Gamma(h_3^0 \rightarrow hh) + \Gamma(h_3^0 \rightarrow gg) + \Gamma(h_3^0 \rightarrow \gamma\gamma) + \Gamma(h_3^0 \rightarrow Z\gamma). \quad (57)$$

The last two decays are calculated as follows,

$$\Gamma(h_3^0 \rightarrow Z\gamma) = \frac{m_{h_3^0}^3}{32\pi} \left(1 - \frac{m_Z^2}{m_{h_3^0}^2} \right)^3 |F_{21}(h_3^0 \rightarrow Z\gamma)|^2, \quad (58)$$

$$\Gamma(h_3^0 \rightarrow \gamma\gamma) = \frac{m_{h_3^0}^3}{64\pi} \times |F_{\gamma\gamma}^{331}(h_3^0 \rightarrow \gamma\gamma)|^2, \quad (59)$$

where

$$\begin{aligned} F_{21}^{331}(h_3^0 \rightarrow Z\gamma) &= \sum_{F=E_a, J_a} F_{21,F}^{331}(h_3^0 \rightarrow Z\gamma) + \sum_s F_{21,s}^{331}(h_3^0 \rightarrow Z\gamma) + \sum_{v=Y,V} F_{21,v}^{331}(h_3^0 \rightarrow Z\gamma) \\ &+ \sum_{\{s,v\}} [F_{21,vs}^{331}(h_3^0 \rightarrow Z\gamma) + F_{21,sv}^{331}(h_3^0 \rightarrow Z\gamma)], \end{aligned} \quad (60)$$

$$F_{\gamma\gamma}^{331}(h_3^0 \rightarrow \gamma\gamma) = \sum_{F=E_a, J_a} F_{\gamma\gamma,F}^{331}(h_3^0 \rightarrow \gamma\gamma) + \sum_s F_{\gamma\gamma,s}^{331}(h_3^0 \rightarrow \gamma\gamma) + \sum_{v=Y,V} F_{\gamma\gamma,v}^{331}(h_3^0 \rightarrow \gamma\gamma),$$

where $s = H^\pm, H^{\pm,A}, H^{\pm,B}$, $v = Y^{\pm,A}, V^{\pm,B}$, and $\{s, v\} = \{H^{\pm,A}, Y^{\pm,A}\}, \{H^{\pm,B}, V^{\pm,B}\}$.

IV. NUMERICAL DISCUSSIONS

A. Significance of the SM-like Higgs decay $h \rightarrow Z\gamma$ under recent constrains of parameters and the decay $h \rightarrow \gamma\gamma$

In this section, many well-known quantities are fixed from experiments [55], namely the SM-like Higgs masses $m_h = 125.09$ GeV, the boson masses m_W, m_Z , masses of well-known fermions, the vev $v \simeq 246$ GeV, the $SU(2)_L$ coupling $g \simeq 0.651$, $\alpha_{\text{em}} = 1/137$, $e = \sqrt{4\pi\alpha_{\text{em}}}$, $s_W^2 = 0.231$.

The unknown independent parameters used as inputs are β , t_{12} , $SU(3)_L$ scale v_3 , the neutral Higgs mixing s_d , the heavy neutral masses $m_{h_2^0}, m_{h_3^0}$, triple Higgs self coupling including $\lambda_1, \tilde{\lambda}_{12}, \tilde{\lambda}_{13}, \tilde{\lambda}_{23}$, and the exotic fermion masses m_{E_a}, m_{J_a} .

To express the differences from the SM, we define a quantity $\delta\mu_X$ ($X = \gamma\gamma, Z\gamma$) as follows

$$\delta\mu_X \equiv (\mu_X - 1) \times 100\%. \quad (61)$$

We also introduce a new quantity $R_{Z\gamma/\gamma\gamma} \equiv |\delta\mu_{Z\gamma}/\delta\mu_{\gamma\gamma}|$ to investigate the relative difference between the two signal strengths, which have many similar properties. The recent allowed values relating with the two photon decay is $-15\% \leq \delta\mu_{\gamma\gamma} \leq 13\%$, corresponding to the recent experimental constraint $\mu_{\gamma\gamma} = 0.99 \pm 0.14$ [4]. The future sensitivities obtained by experiments we accept here are $\mu_{\gamma\gamma} = 1 \pm 0.04$ and $\mu_{Z\gamma} = 1 \pm 0.23$ [9], i.e. $|\delta\mu_{\gamma\gamma}| \leq 4\%$ and $|\delta\mu_{Z\gamma}| \leq 23\%$, respectively.

The $SU(3)_L$ scale depends strongly on the heavy neutral gauge boson mass $m_{Z'}$, which the lower bound is constrained from experimental searches for decays to pairs of SM leptons $Z' \rightarrow \ell\bar{\ell}$, particular reports for 3-3-1 models, see [66] where decays to exotic lepton pairs are included. Accordingly, at LHC@14TeV, $m_{Z'} < 4$ TeV is excluded at the integrated luminosity of 23 fb^{-1} for $\beta = -1/\sqrt{3}$. Because $v_3 \sim \mathcal{O}(1)$ TeV, the $m_{Z'}$ is approximately $m_{Z'}^2 = \frac{g^2 v_3^2 c_W^2}{3[1-(1+\beta^2)s_W^2]}$. Recent works used $m_{Z'} \geq 4$ TeV for models with $\beta = -1/\sqrt{3}$ [67, 68], based on the latest LHC search [69–71]. This lower bound of $m_{Z'}$ corresponds to lower bounds of $v_3 \geq 10.6, 10.1, 8.2, 3.3$ TeV corresponding to $\beta = 0, \pm 1/\sqrt{3}, \pm 2/\sqrt{3}, \pm \sqrt{3}$. Recent discussion on 3-3-1 models with heavy right-handed neutrinos where $\beta = -1/\sqrt{3}$ and $m_{Z'} = 3$ TeV is allowed [72, 73] because the decay of Z' into a pair of light exotic neutrinos is included. The respective lower bound of the $SU(3)_L$ scale is $v_3 \geq 7.6$ TeV, which is still the same mentioned bounds. On the other hand, a model with $\beta = \sqrt{3}$ still allows rather low $SU(3)_L$ scale, for example $m_{Z'} \simeq 3.25$ TeV, corresponding to $v_3 \simeq 2.7$ TeV [74].

In investigating the h_3^0 decays, we can put $m_{E_a} = m_{J_a} = m_F$. There is a more general case that the mixing between different exotic leptons appear, then the loop with two distinguished fermions will contribute to the $h_3^0 \rightarrow Z\gamma$ decay amplitude only.

The perturbative limits require that the absolute values of all Yukawa and Higgs self couplings should be less than $\sqrt{4\pi}$ and 4π , respectively. This leads to the constraint of the t_{12} from the Yukawa coupling of the top quark in Eq. (9), namely $t_{12} < \sqrt{2\pi}v/m_t \simeq 3.5$. Other studies on the 2HDM suggests that $t_{12} > 1/60$ [9]. We will limit that $0.1 \leq t_{12} \leq 3$, which is consistent with ref. [1] and allow large $|s_\theta| \geq 5 \times 10^{-3}$.

Considering $m_{h_2^0}, m_A, m_{H^\pm}, t_{12}$ and s_δ as parameters of a 2HDM model mentioned in ref. [11], important constraints can be found as $c_\delta > 0.99$ for all 2HDMs, leading to rather large range of $|s_\delta| < 0.14$. But large s_δ prefer that t_{12} is around 1 [76]. The recent global fit for 2HDM give the same result [77]. Lower masses of heavy Higgs bosons are around 1 TeV. As we will show, the recent signal strength of the SM-like Higgs decay $h \rightarrow \gamma\gamma$ gives more strict constraint on s_θ , hence we focus on the interesting range $|s_\theta| \leq 0.05$. The parameters relating with 2HDM λ_2 and λ_{12} affect strongly on $m_{h_2^0}$. Large $|s_\theta|$ results in small allowed values of $m_{h_2^0}$ in order to keep λ_{12} satisfying the perturbative limit. In contrast, all other quantities relating with the $SU(3)_L$ symmetry are well allowed. The regions of parameter space chosen here are consistent with the recent works on 2HDM [78–80]. The recent experimental searches for Higgs bosons predicted by 2HDM have been paid

much attentions [81]. The value of 300 GeV for lower bounds of charged and CP-even neutral Higgs bosons are accepted in recent studies on 2HDM [80]. Following that, values of $m_{h_2^0}$ and m_{H^\pm} are always chosen to satisfy that $m_{h_2^0}, m_{h_2^\pm} \geq 300$ GeV.

The default values of unknown independent parameters we choose here are $\beta = 1/\sqrt{3}$, $s_\delta = 0.01$, $\lambda_1 = 1$, $t_{12} = 0.8$, $\tilde{\lambda}_{12} = \tilde{\lambda}_{13} = \tilde{\lambda}_{23} = 0.1$, $m_{h_2^0} = 1.2$ TeV, $m_{h_3^0} = 1$ TeV, $v_3 = 14$ TeV, $m_{E_a} = m_{J_a} = 1.5$ TeV. Depending on the particular discussions, changing any numerical values will be noted.

We will also consider the case of light charged Higgs masses, which loop contributions to the decay $h \rightarrow \gamma\gamma, Z\gamma$ may be large. Accordingly, the Higgs self couplings $\tilde{\lambda}_{ij}$ relating with charged Higgs masses in Eqs. (22), (23) and (24), should be negative. Our investigation suggests that $|\tilde{\lambda}_{13,23}| \leq \mathcal{O}(10^{-3})$ while $|\tilde{\lambda}_{12}|$ can be reach order 1. We will consider more detailed in particular numerical investigations.

Strict constraints of the Higgs-self couplings for a 3-3-1 model with right handed neutrino were discussed in ref. [51], where the Higgs potential is forced to satisfy the vacuum stability condition. Accordingly, interesting results can be applied to the 3-3-1 models with arbitrary β , namely

$$\lambda_i > 0, \quad f_{ij} \equiv \lambda_{ij} + 2\sqrt{\lambda_i \lambda_j} > 0, \quad \tilde{f}_{ij} \equiv \lambda_{ij} + \tilde{\lambda}_{ij} + 2\sqrt{\lambda_i \lambda_j} > 0, \quad (62)$$

with $i, j = 1, 2, 3$ and $i < j$. Note that the constraints on the Higgs self-couplings $\lambda_{1,2,12}$ correspond to the particular cases of the 2HDM [11, 55, 75]. Because $(t_{12} + t_{12}^{-1} + c_{12}(v/v_3)^2) f v_3 \sim m_A^2$ being the squared mass of the CP-odd neutral Higgs boson, the requirement $m_A^2 > 0$ shows $f > 0$ [1, 82]. The other conditions guarantee that all squared Higgs masses must be positive and SM-like Higgs mass is identified with the experimental value. It can be seen in Eqs. (22)-(24) that all charged Higgs squared masses are always positive if all $\tilde{\lambda}_{ij} > 0$, but their values seem very large. More interesting cases correspond to the existence of light charged Higgs bosons, which may contribute significant contributions to loop-induced decays of the SM-like Higgs bosons. Based on eq. (26), a first estimation suggests that f has the same order with $SU(3)_L$ scale v_3 , leading to the requirement that $\tilde{\lambda}_{12,13,23} < 0$ for the existence of light charged Higgs bosons. Furthermore, the relation (34) results in a consequence that λ_{13} will be small for the case of our interest with large $v_3 \geq 3$ TeV and small $m_{h_2^0}$ around 1 TeV. In this case f is also small, as we realize in the numerical investigation as well as it has been shown recently [85]. Taking this into

account to the charged Higgs masses in Eqs.(23) and (24) we derive that the absolute values of negative values of $\tilde{\lambda}_{13,23}$ seems very small. In contrast, the appearance of a light charged Higgs H^\pm allows negative $\tilde{\lambda}_{12}$ and rather large $|\tilde{\lambda}_{12}|$ that satisfy the inequality $\tilde{f}_{12} > 0$ given in (62). We will consider the two separate cases: $\tilde{\lambda}_{ij} \geq 0$ with all $i > j$, $i, j = 1, 2, 3$; and $\tilde{\lambda}_{12} < 0$. The values of $\lambda_{13,23}$ are always chosen to get large absolute values of $F_{21,s}^{331}$, and/or $F_{21,sv}^{331} \equiv F_{21,svv}^{331} + F_{21,vss}^{331}$.

1. Case 1: $\tilde{\lambda}_{12} \geq 0$

First, we focus on the 2HDM parameters. Figures 2 and 3 illustrate numerically Higgs-self couplings and f_{ij} as functions of $m_{h_2^0}$, and other independent parameters are fixed as $t_{12} = 0.8$ and changing $s_\delta = \pm 10^{-2}, \pm 5 \times 10^{-2}$, which are significantly large. For $s_\delta > 0$, the

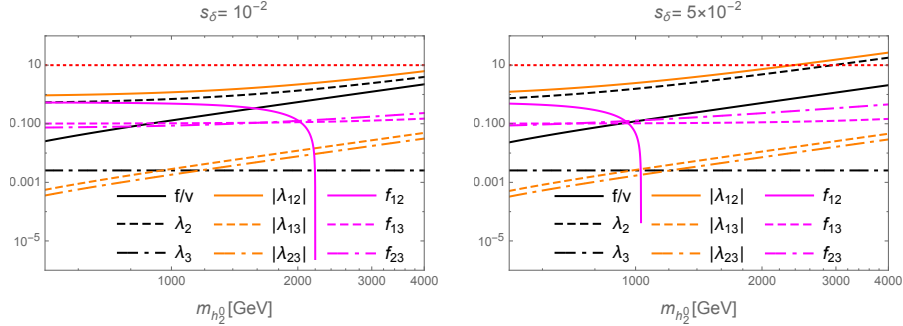


FIG. 2: f_{ij} and Higgs self couplings as functions of $m_{h_2^0}$ with $s_\delta > 0$ and $t_{12} = 0.8$.

t_{12} is chosen large enough to satisfy $f_{12} > 0$ and $m_{h_2^0} > 1$ TeV. The parameters $\tilde{\lambda}_{12} \geq 0$ and negative $\tilde{\lambda}_{13,23} \rightarrow 0$ do not affect the quantities investigated in this figure. We conclude that the vacuum stability requirement $f_{12} > 0$ gives strong upper bound on $m_{h_2^0}$, where larger s_δ give small allowed $m_{h_2^0}$.

Figure 3 illustrates allowed regions for $s_\delta < 0$, where we choose $t_{12} = 0.1$, enough small to allow $\lambda_2 > 0$ and $m_{h_2^0} > 1$ TeV. Again we derive that larger $|s_\delta|$ gives smaller upper bound of $m_{h_2^0}$.

In general, our scan shows that allowed t_{12} and s_θ are affected the most strongly by $m_{h_2^0}$. As illustration, the figure 4 presents allowed regions of t_{12} and s_θ with two fixed $m_{h_2^0} = 1$ TeV and 2.5 TeV. It can be seen that larger $m_{h_2^0}$ results in smaller allowed $|s_\theta|$. The dashed black curves presenting constant values of f_{12} will be helpful for the discussion on the case

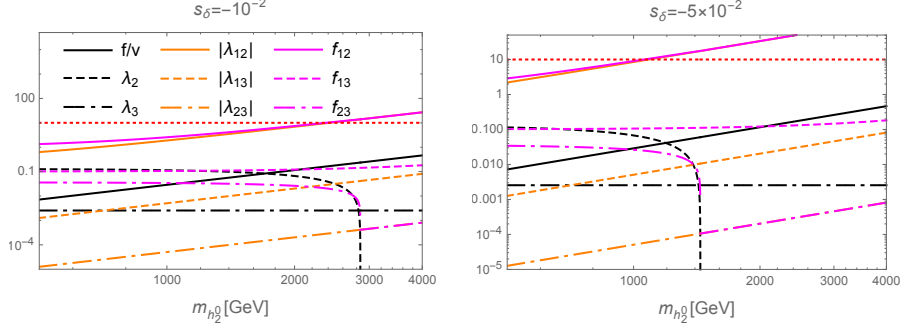


FIG. 3: f_{ij} and Higgs self couplings as functions of $m_{h_2^0}$ with $s_\delta < 0$ and $t_{12} = 0.1$.

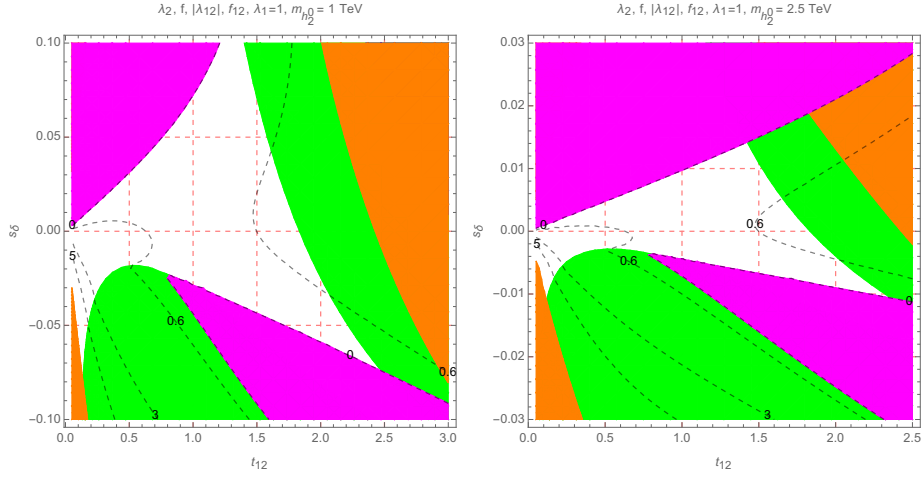


FIG. 4: Contour plots of λ_2 , f , $|\lambda_{12}|$ and f_{12} as functions of s_θ and t_{12} . The green, blue, orange, magenta regions are excluded by requirements that $0 < \lambda_2 < 10$, $f > 0$, $|\lambda_{12}| < 10$, and $f_{12} > 0$, respectively. Dashed-black curves present constant values of f_{12} .

of $\tilde{\lambda}_{12} < 0$. This is because the constraint from $\tilde{f}_{12} > 0$ will be more strict than that from $f_{12} > 0$ when $\tilde{\lambda}_{12} < 0$, namely it will be equivalent to $f_{12} > |\tilde{\lambda}_{12}|$. Hence f_{12} plays role as the upper bound of $|\tilde{\lambda}_{12}|$.

The allowed regions also depend on λ_1 , see contour plots in figure 5 corresponding to $\lambda_1 = 0.5, 5$. It can be seen that λ_1 should be large enough to allow large $|s_\theta|$, see illustrations in fig. 12 for $\lambda_1 = 0.1, 10$ in appendix C.

In the case of large $|s_\theta| = 0.02$, the allowed values λ_1 and t_{12} are shown in figure 6. It can be seen that only negative s_θ allows large f_{12} . The case of larger $|s_\theta| = 0.05$ is shown in fig. 13 of the appendix C. We can choose $m_{h_2^0} = 1.2$ TeV so that $|s_\theta| = 0.05$ is still allowed. Both large $|s_\delta|$ and $m_{h_2^0}$ give narrow allowed regions of t_{12} and λ_1 , and small f_{12} . For small $|s_\delta| < 10^{-2}$, the allowed values of $m_{h_2^0}$ and t_{12} will relax. But it will not result in much

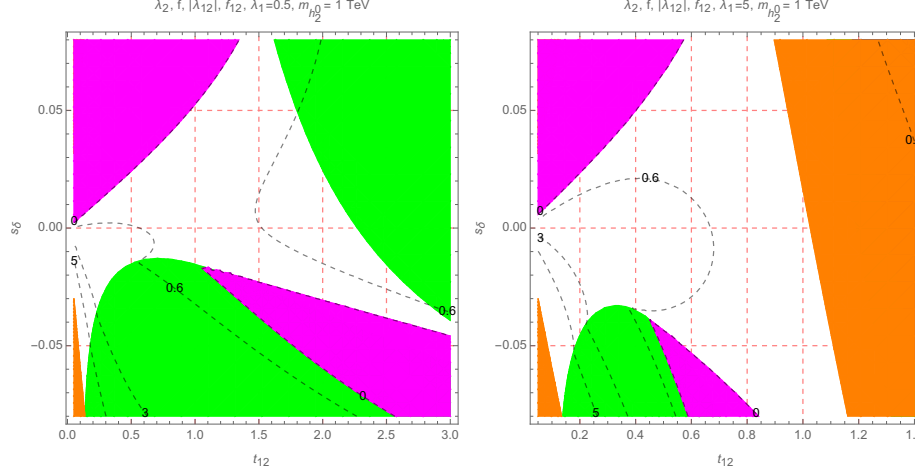


FIG. 5: Contour plots of λ_2 , $|\lambda_{12}|$ and f_{12} as functions of s_δ and t_{12} . The green, blue, orange, magenta regions are excluded by requirements that $0 < \lambda_2 < 10$, $f > 0$, $|\lambda_{12}| < 10$, and $f_{12} > 0$, respectively. Dashed-black curves presents constant values of f_{12} .

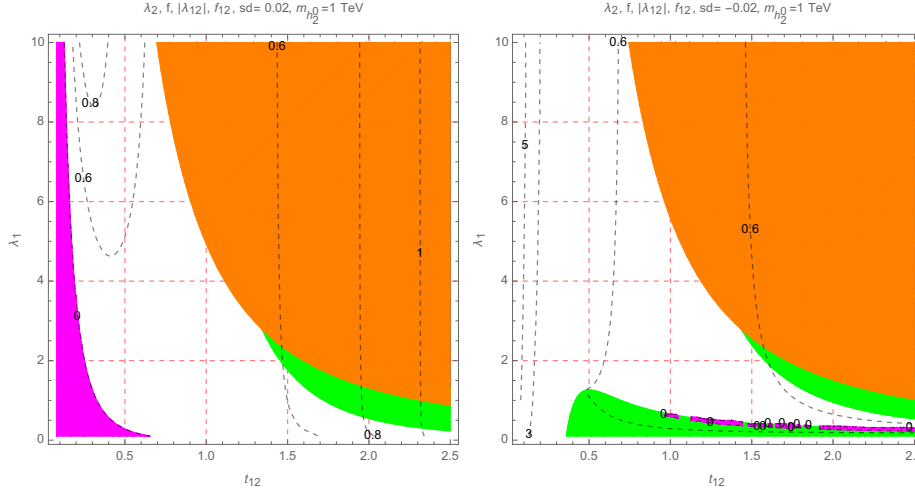


FIG. 6: Contour plots of λ_2 , $|\lambda_{12}|$ and f_{12} as functions of λ_1 and t_{12} with some fixed $m_{h_2^0}$. The green, blue, orange, magenta regions are excluded by requirements that $0 < \lambda_2 < 10$, $f > 0$, $|\lambda_{12}| < 10$, and $f_{12} > 0$, respectively. Dashed-black curves present constant values of f_{12} .

deviation from the SM prediction.

The left panel of Figure 7 illustrates the contour plots with fixed $\beta = -1/\sqrt{3}$ for allowed values of $\delta\mu_{Z\gamma}$ corresponding to the none-color regions that satisfy the constraints of parameters and the recent experimental bound on $\delta\mu_{\gamma\gamma}$. The right panel of Figure 7 shows the contour plots of $R_{Z\gamma/\gamma\gamma}$, where the non color region satisfies $R_{Z\gamma/\gamma\gamma} \geq 2$. In this region, we can see that $|s_\delta| \sim \mathcal{O}(10^{-3})$ and negative. Hence, the current constraints $\mu_{\gamma\gamma} = 0.99 \pm 0.14$

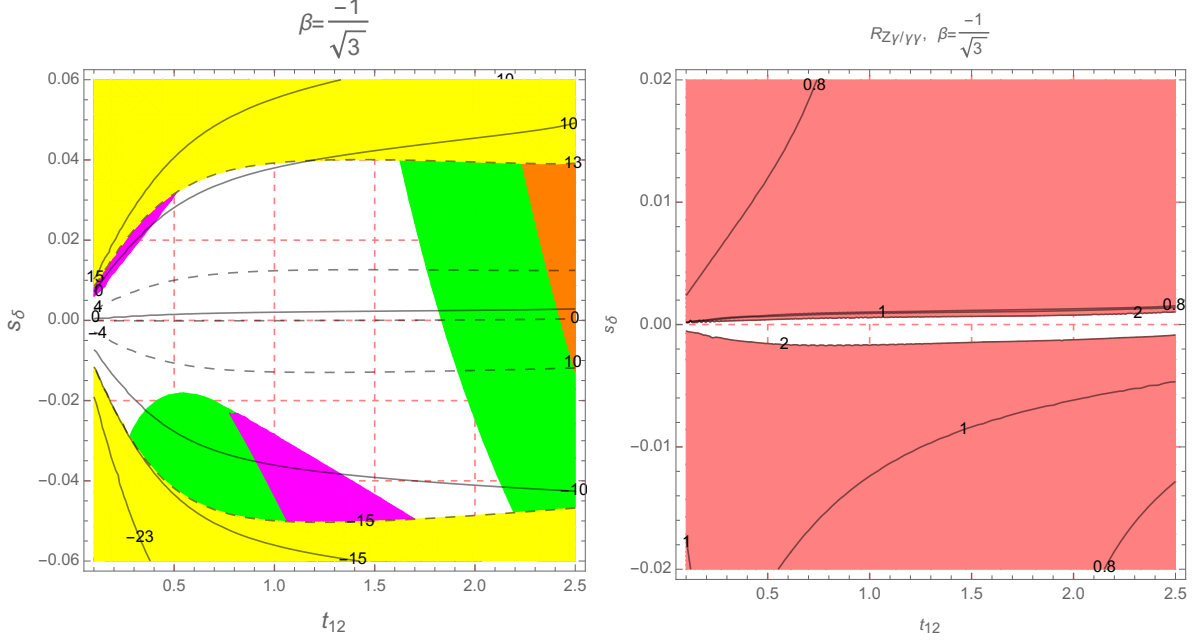


FIG. 7: Contour plots showing allowed regions of s_δ and t_{12} (left) and $R_{Z\gamma/\gamma\gamma}$ as a function of s_δ and t_{12} . The green, blue, orange, magenta and yellow regions are excluded by valid requirements of $\lambda_2, f, \lambda_{12}, f_{12}$, and $\delta\mu_{\gamma\gamma}$, respectively. The black and dotted black curves show constant values of $\delta\mu_{Z\gamma}$ and $\delta\mu_{\gamma\gamma}$, respectively. The non color region in the right panel corresponds to $R_{Z\gamma/\gamma\gamma} \geq 2$.

predicts $|\delta\mu_{Z\gamma}| < 0.15$ which is still smaller than the future sensitivity $\delta\mu_{Z\gamma} = \pm 0.23$ mentioned in ref. [9]. In addition, most of the allowed regions satisfy $0.8 \leq R_{Z\gamma/\gamma\gamma} \leq 2$, hence the approximation $\text{Br}(h \rightarrow \gamma\gamma) \simeq \text{Br}(h \rightarrow Z\gamma)$ is accepted for simplicity in previous works.

For large $v_3 = 14$ TeV and recent uncertainty of the $\delta\mu_{\gamma\gamma}$, our investigation shows generally that the above discussions on the allowed regions as well as $R_{Z\gamma/\gamma\gamma}$ illustrated in figure 7 depend weakly on β . The results are also unchanged for lower bound of $v_3 = 8$ TeV which is allowed for $\beta = \pm 2/\sqrt{3}$. This property can be explained by the fact that, large $v_3 \simeq 10$ TeV results in heavy charged gauge bosons m_Y, m_V having masses around 4 TeV, and the charged Higgs masses not less than 1 TeV. As a by product, one loop contributions from $SU(3)_L$ particles to F_{21}^{331} and $F_{\gamma\gamma}^{331}$ are at least four orders smaller than the corresponding SM amplitudes $F_{21,\gamma\gamma}^{\text{SM}}$, illustrations are given in table VIII. Here we use the SM amplitudes predicted by the SM, namely $\text{Re}[F_{21}^{\text{SM}}] = -5.6 \times 10^{-5} [\text{GeV}^{-1}]$ and $\text{Re}[F_{\gamma\gamma}^{\text{SM}}] = -3.09 \times 10^{-5} [\text{GeV}^{-1}]$, and ignore the tiny imagine parts. We can see that both $\delta_{Z\gamma}$ and $\delta_{\gamma\gamma}$ depend strongly on s_δ and t_{12} . In contrast, the one-loop contributions from new particles are suppressed, as shown in the last line in table VIII: suppressed s_δ results in $|\delta\mu_{Z\gamma}| \simeq 4|\delta\mu_{\gamma\gamma}| = 0.8 \ll 4$,

β	s_δ	t_{12}	$\frac{F_{21,s}^{331}}{\text{Re}[F_{21}^{\text{SM}}]}$	$\frac{F_{21,v}^{331}}{\text{Re}[F_{21}^{\text{SM}}]}$	$\frac{F_{21,sv}^{331}}{\text{Re}[F_{21}^{\text{SM}}]}$	$\frac{F_{\gamma\gamma,s}^{331}}{\text{Re}[F_{\gamma\gamma}^{\text{SM}}]}$	$\frac{F_{\gamma\gamma,v}^{331}}{\text{Re}[F_{\gamma\gamma}^{\text{SM}}]}$	$\delta\mu_{Z\gamma}$	$\delta\mu_{\gamma\gamma}$
$\frac{2}{\sqrt{3}}$	2×10^{-2}	1.5	-3.3×10^{-4}	3×10^{-5}	-1.6×10^{-4}	-6×10^{-4}	5.5×10^{-4}	4.4	6.5
$\frac{2}{\sqrt{3}}$	-2×10^{-2}	1.5	$\sim 10^{-6}$	3×10^{-5}	-1.5×10^{-4}	$\sim 10^{-6}$	5.3×10^{-4}	-5.4	-6
$\frac{2}{\sqrt{3}}$	2×10^{-2}	0.5	1.3×10^{-4}	-9×10^{-5}	-5×10^{-5}	2.3×10^{-4}	2.2×10^{-4}	6.8	8.1
$\frac{2}{\sqrt{3}}$	-2×10^{-2}	0.5	-4.2×10^{-4}	-9×10^{-5}	-4×10^{-5}	-7.5×10^{-4}	2.1×10^{-4}	-7.5	-7.4
$\frac{2}{\sqrt{3}}$	-10^{-3}	1.5	-1.6×10^{-4}	3×10^{-5}	-1.6×10^{-4}	-2.9×10^{-4}	5.4×10^{-4}	-0.8	-0.2

TABLE VIII: Numerical contributions of $SU(3)_L$ particles to F_{21}^{331} and $F_{\gamma\gamma}^{331}$, see Eqs. (42) and (44), where $F_{21,sv}^{331} \equiv F_{21,svv}^{331} + F_{21,vss}^{331}$.

which is even much smaller than the expected sensitivity of $\delta\mu_{\gamma\gamma} = 4$. Anyway, it can be noted that $F_{21,sv}^{331}$ may significantly larger than $F_{21,v}^{331}$, hence both of them should be included simultaneously into the decay amplitude $h \rightarrow Z\gamma$ in general. Suppressed contributions of new particles to $\delta\mu_{Z\gamma}$, are shown explicitly in the left panel of figure 7, where three lines of $s_\delta = \delta_{Z\gamma} = \delta_{\gamma\gamma} = 0$ are very close together.

For large and positive $\tilde{\lambda}_{12}$ and small $m_{h_2^0}$, one loop contributions from H^\pm to F_{21}^{331} and $F_{\gamma\gamma}^{331}$ are dominant but still not large enough to give significant deviations to $\delta\mu_{Z\gamma}$, see illustration with suppressed $s_\delta = 10^{-3}$ in the first line of table IX. Here we always force

β	s_δ	t_{12}	$\frac{F_{21,s}^{331}}{\text{Re}[F_{21}^{\text{SM}}]}$	$\frac{F_{21,v}^{331}}{\text{Re}[F_{21}^{\text{SM}}]}$	$\frac{F_{21,sv}^{331}}{\text{Re}[F_{21}^{\text{SM}}]}$	$\frac{F_{\gamma\gamma,s}^{331}}{\text{Re}[F_{\gamma\gamma}^{\text{SM}}]}$	$\frac{F_{\gamma\gamma,v}^{331}}{\text{Re}[F_{\gamma\gamma}^{\text{SM}}]}$	$\delta\mu_{Z\gamma}$	$\delta\mu_{\gamma\gamma}$
$\frac{2}{\sqrt{3}}$	10^{-3}	1.7	-1.46×10^{-2}	4×10^{-5}	-1.7×10^{-4}	-2.64×10^{-2}	5.7×10^{-4}	-3.1	-4.7
$\frac{2}{\sqrt{3}}$	-10^{-3}	1.7	-1.44×10^{-2}	4×10^{-5}	-1.7×10^{-4}	-2.61×10^{-2}	5.7×10^{-4}	-3.6	-5.3
$\frac{2}{\sqrt{3}}$	3×10^{-2}	1.5	-1.24×10^{-2}	3×10^{-5}	-1.6×10^{-4}	-2.23×10^{-2}	5.5×10^{-4}	4.4	5.2
$\frac{2}{\sqrt{3}}$	-3×10^{-2}	1.5	-9.6×10^{-3}	3×10^{-5}	-1.5×10^{-4}	-1.75×10^{-3}	5.3×10^{-4}	-9.6	-12.3

TABLE IX: Numerical contributions of $SU(3)_L$ particles to F_{21}^{331} and $F_{\gamma\gamma}^{331}$ for large $\tilde{\lambda}_{12} = 5$ and small $m_{h_2^0} = 600$ GeV.

$|\delta\mu_{\gamma\gamma}| \leq 4\%$ being the future sensitive of $\mu_{\gamma\gamma}$. On the other hand, large deviations can result from large $|s_\delta|$. In this case, all $\delta_{Z\gamma,\gamma\gamma}$ and s_δ have the same signs.

Regarding $\beta = \sqrt{3}$ corresponding to the model discussed in ref. [74], where $v_3 = 3$ TeV is still accepted, the allowed regions changes significantly, as illustrated in figure 8. In particularly, the model gives more strict positive $s_\delta < 0.03$. one-loop contributions from $SU(3)_L$ particles can give deviations up to few percent for both $\delta\mu_{Z\gamma}$, $\delta\mu_{\gamma\gamma}$. This property

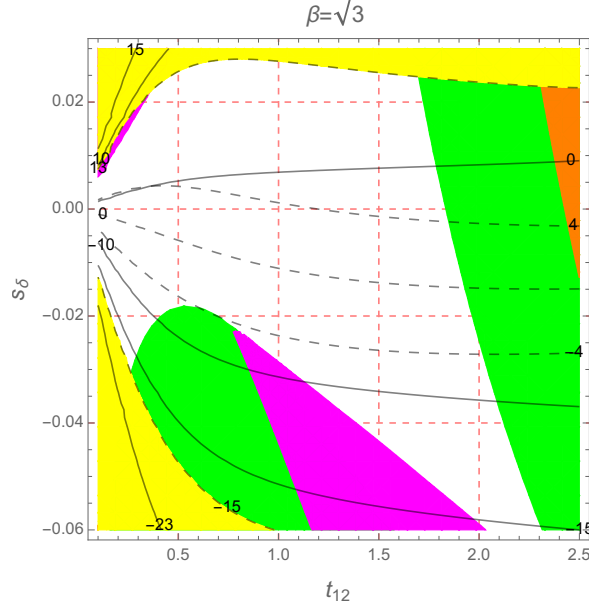


FIG. 8: Contour plots showing allowed regions of s_δ and t_{12} with $v_3 = 3$ TeV following ref. [74]. The green, blue, orange, magenta and yellow regions are excluded by valid requirements of $\lambda_2, f, \lambda_{12}, f_{12}$, and $\delta\mu_{\gamma\gamma}$, respectively. The black and dotted black curves show constant values of $\delta\mu_{Z\gamma}$ and $\delta\mu_{\gamma\gamma}$, respectively.

is shown in the left panel of figure 8 that the two contours $\delta_{Z\gamma} = \delta_{\gamma\gamma} = 0$ distinguish with the line $s_\delta = 0$. Interesting numerical values are illustrated in table X. We emphasize two

β	s_δ	t_{12}	$\frac{F_{21,s}^{331}}{\text{Re}[F_{21}^{\text{SM}}]}$	$\frac{F_{21,v}^{331}}{\text{Re}[F_{21}^{\text{SM}}]}$	$\frac{F_{21,sv}^{331}}{\text{Re}[F_{21}^{\text{SM}}]}$	$\frac{F_{\gamma\gamma,s}^{331}}{\text{Re}[F_{\gamma\gamma}^{\text{SM}}]}$	$\frac{F_{\gamma\gamma,v}^{331}}{\text{Re}[F_{\gamma\gamma}^{\text{SM}}]}$	$\delta\mu_{Z\gamma}$	$\delta\mu_{\gamma\gamma}$
$\sqrt{3}$	10^{-3}	1.5	-1.8×10^{-4}	-1.6×10^{-3}	-4×10^{-3}	-3.2×10^{-4}	2.2×10^{-2}	-1.6	4.8
$\sqrt{3}$	-10^{-3}	1.5	-1.6×10^{-4}	-1.7×10^{-3}	-4×10^{-3}	-2.9×10^{-4}	2.2×10^{-2}	-2	4.2

TABLE X: For model in ref. [74], numerical contributions of $SU(3)_L$ particles to F_{21}^{331} and $F_{\gamma\gamma}^{331}$. Notations are given from caption of table VIII.

important properties. First, one loop contributions from gauge $SU(3)_L$ bosons are dominant, which can give $\delta\mu_{\gamma\gamma}$ to reach the future sensitivity. Values of $F_{21,v}^{331}$ and $F_{21,v}^{331}$ can have the same order of 10^{-3} compared with the SM part, but these contributions are not large enough to result in large deviation of $|\delta\mu_{Z\gamma}| > 23\%$.

To finish the case of $\lambda_{ij} > 0$ we mentioned above, we see that in this case all of the charged Higgs boson masses are order of $O(1)\text{TeV}$ and small couplings with h_1^0 . For large λ_1, λ_{12} and small $m_{h_2^0} = 800$ GeV, there may give small $\delta\mu_{\gamma\gamma}$ but large $\delta\mu_{Z\gamma}$, see examples

in table XI. We will show here an interesting point that with the existence of new Higgs and

λ_1	$\tilde{\lambda}_{12}$	s_δ	t_{12}	$\frac{F_{21,s}^{331}}{\text{Re}[F_{21}^{\text{SM}}]}$	$\frac{F_{21,v}^{331}}{\text{Re}[F_{21}^{\text{SM}}]}$	$\frac{F_{21,sv}^{331}}{\text{Re}[F_{21}^{\text{SM}}]}$	$\frac{F_{\gamma\gamma,s}^{331}}{\text{Re}[F_{\gamma\gamma}^{\text{SM}}]}$	$\frac{F_{\gamma\gamma,v}^{331}}{\text{Re}[F_{\gamma\gamma}^{\text{SM}}]}$	$\delta\mu_{Z\gamma}$	$\delta\mu_{\gamma\gamma}$
1.95	8	10^{-3}	1.5	-1.22×10^{-2}	-1.7×10^{-3}	-4.4×10^{-3}	-2.21×10^{-2}	2.2×10^{-2}	-4.	0.4
1.95	8	-10^{-3}	1.5	-1.21×10^{-2}	-1.7×10^{-3}	-4.4×10^{-3}	-2.19×10^{-2}	2.2×10^{-2}	-4.5	-0.17
1.	5	-2×10^{-2}	1.95	-1.6×10^{-3}	-9.7×10^{-4}	-5×10^{-3}	-1.2×10^{-2}	2.4×10^{-2}	-7.7	-4

TABLE XI: For model in ref. [74], numerical contributions of $SU(3)_L$ particles to F_{21}^{331} and $F_{\gamma\gamma}^{331}$ with $m_{h_2^0} = 800$ GeV. Notations are given from caption of table VIII.

gauge bosons, their contributions $F_{\gamma\gamma,s}^{331}$ and $F_{\gamma\gamma,v}^{331}$ to the decay amplitude $h_1^0 \rightarrow \gamma\gamma$ can be destructive, hence keep the respective signal strength satisfying the experimental constraint. Simultaneously, all of the contribution to the decay amplitude $h_1^0 \rightarrow Z\gamma$ are constructive so that the deviation can be large. For the model with $\beta = \sqrt{3}$ and $v_3 = 3$ TeV, we can find this deviation can reach around -10 , but this values is still far from the expected sensitive $\delta\mu_{Z\gamma} = \pm 23\%$ in the HL-LHC project. For the models with $v_3 \geq 8$ TeV, gauge contributions are suppressed, hence large contribution from charged Higgs bosons is dominant. Then, the constraint from $\delta\mu_{\gamma\gamma}$ will give more strict constraint on $\delta\mu_{Z\gamma}$.

2. Case 2: $\tilde{\lambda}_{12} < 0$.

As we can see in eq. (22), negative $\tilde{\lambda}_{12}$ may result in small charged Higgs mass H^\pm . In addition, large $|\tilde{\lambda}_{12}|$ may give large coupling of this Higgs boson with the SM-like one, leading to large $|F_{21,s}^{331}|$ and $|F_{\gamma\gamma,s}^{331}|$. We will focus on this interesting case.

One of the conditions given in (62), namely $\tilde{f}_{12} > 0$, which is satisfied automatically if $f_{12} > 0$ and $\tilde{\lambda}_{12} \geq 0$. In the case of $\tilde{\lambda}_{12} < 0$, the inequality $\tilde{f}_{12} > 0$ is equivalent to the more strict condition $f_{12} > |\tilde{\lambda}_{12}| > 0$ or $-f_{12} < \tilde{\lambda}_{12} < 0$. This helps us determine the allowed regions with large $|\tilde{\lambda}_{12}|$, which give large one-loop contributions of charged Higgs boson H^\pm to the two decay amplitudes $h \rightarrow Z\gamma, \gamma\gamma$. Based on the fact that allowed regions with large positive f_{12} will allow large $\tilde{\lambda}_{12}$, two figures 4 and 5 show that large $\tilde{\lambda}_{12}$ corresponds to regions having negative s_δ and small t_{12} . Small s_θ allows small $|\tilde{\lambda}_{12}|$. The figure 6 shows that values of λ_1 seems not affect allowed $\tilde{\lambda}_{12}$ in the regions of negative s_δ . For large v_3 , large $|\tilde{\lambda}_{12}|$ in this case does not affect significantly on both $\delta\mu_{Z\gamma, \gamma\gamma}$ see illustration in table XII.

Hence, the case of negative $\tilde{\lambda}_{12}$ may results in light charged Higgs boson H^\pm , but it not

β	$m_{h_2^0}$ [TeV]	s_δ	$\frac{F_{21,s}^{331}}{F_{21}^{\text{SM}}}$	$\frac{F_{21,v}^{331}}{F_{21}^{\text{SM}}}$	$\frac{F_{21,sv}^{331}}{F_{21}^{\text{SM}}}$	$\frac{F_{\gamma\gamma,s}^{331}}{F_{\gamma\gamma}^{\text{SM}}}$	$\frac{F_{\gamma\gamma,v}^{331}}{F_{\gamma\gamma}^{\text{SM}}}$	$\delta\mu_{Z\gamma}$	$\delta\mu_{\gamma\gamma}$
$\frac{2}{\sqrt{3}}$	1	-10^{-3}	3.4×10^{-4}	-1.4×10^{-4}	$\simeq 0$	6.1×10^{-3}	9×10^{-5}	-1.8	-1.2
$\frac{2}{\sqrt{3}}$	0.6	-10^{-3}	1.2×10^{-3}	-1.4×10^{-4}	$\simeq 0$	-2.1×10^{-3}	9×10^{-5}	-1.7	-0.9
$\frac{2}{\sqrt{3}}$	1	-2×10^{-2}	-1.4×10^{-3}	-1.4×10^{-4}	$\simeq 0$	-2.6×10^{-3}	9×10^{-5}	-23.9	-23.9
$\frac{2}{\sqrt{3}}$	0.6	-2×10^{-2}	6.6×10^{-4}	-1.2×10^{-3}	$\simeq 0$	-1.2×10^{-3}	9×10^{-5}	-23.7	-23.6

TABLE XII: Numerical contributions of $SU(3)_L$ particles to F_{21}^{331} and $F_{\gamma\gamma}^{331}$. Numerical fixed values of unknown parameters are: $\beta = 2/\sqrt{3}$, $t_{12} = 0.1$, $\tilde{\lambda}_{12} = -1$.

supports large one-loop contributions from charged Higgs mediation to decay amplitudes $h \rightarrow Z\gamma, \gamma\gamma$.

Regarding the model with $\beta = \sqrt{3}$ discussed in ref. [74], the main difference is the small $v_3 = 3$ TeV, leading to a significant of heavy gauge bosons to one-loop contribution of loop induced decays $|F_{21,v}^{331}/F_{21}^{\text{SM}}|$, $|F_{21,sv}^{331}/F_{21}^{\text{SM}}|$, $|F_{21,s}^{331}/F_{21}^{\text{SM}}|$, $|F_{\gamma\gamma,v}^{331}/F_{\gamma\gamma}^{\text{SM}}|$, $|F_{\gamma\gamma,v}^{331}/F_{\gamma\gamma}^{\text{SM}}| \sim \mathcal{O}(10^{-2})$. But with $\tilde{\lambda}_{12} < 0$, constructive contributions appear in the decay amplitude $h \rightarrow \gamma\gamma$, while destructive contributions appear in the decay amplitude $h \rightarrow Z\gamma$. Hence, the constraint from experimental data of the decay $h \rightarrow \gamma\gamma$ predicts smaller deviation of the $\mu_{Z\gamma}$ that that corresponding to $\tilde{\lambda}_{12} > 0$.

To finish, from above discussion we emphasize that in other gauge extensions from the SM such as the $SU(2)_1 \otimes SU(2)_2 \otimes U(1)_Y$ models, which still allow low values of new gauge and charged Higgs bosons masses [64, 88–91], the contributions like $F_{12,sv}$ may be as large as usual ones, hence it should be included in the decay amplitude $h \rightarrow Z\gamma$. In addition, these models may predict large $\delta\mu_{Z\gamma}$ which also satisfy $|\delta\mu_{\gamma\gamma}| \leq 0.04$. This interesting topic deserves to be paid attention more detailed.

B. h_3^0 decays as a significance of 3-3-1 models

Different contributions to loop-induced decays $h_3^0 \rightarrow \gamma\gamma, Z\gamma$ with small $s_\theta = 10^{-3}$, $m_{h_3^0} = 700$ GeV, $t_{12} = 0.8$ are illustrated in figure 9, where the ratios $|F_{21,x}(h_3^0 \rightarrow Z\gamma)|/|F_{21}(h_3^0 \rightarrow Z\gamma)|$ and $|F_{\gamma\gamma,x}(h_3^0 \rightarrow Z\gamma)|/|F_{\gamma\gamma}(h_3^0 \rightarrow Z\gamma)|$ are presented, $x = f, s, v, sv$. In addition, our scan shows that the curves in the figure 9 do not sensitive with the changes of s_δ . We

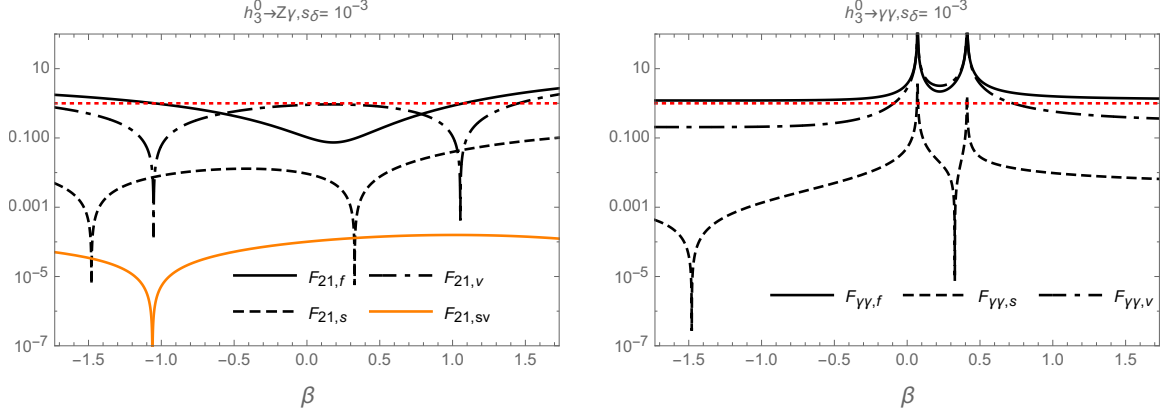


FIG. 9: Different contributions to loop-induced decays $h_3^0 \rightarrow \gamma\gamma, Z\gamma$ as functions of β .

can conclude that contributions from heavy exotic fermions are always dominant for large β . While $F_{21,sv}$ is suppressed. For the decay $h_3^0 \rightarrow \gamma\gamma$, the destructive correlation between $F_{\gamma\gamma,v}$ and $F_{\gamma\gamma,f}$ happens with small $|\beta|$. This results in two peaks in the figure, where $|F_{\gamma\gamma}| \ll |F_{\gamma\gamma,f}|, |F_{\gamma\gamma,v}|$.

Individual branching ratios of h_3^0 are shown in figure 10. The most interesting property

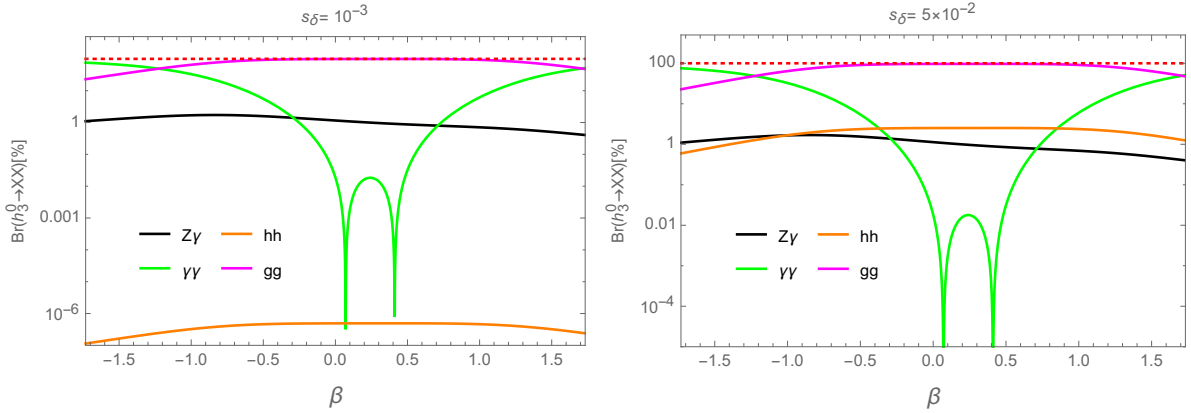


FIG. 10: Branching ratios of the h_3^0 decays as functions of β .

is that, the $\text{Br}(h_3^0 \rightarrow \gamma\gamma)$ may have large values and it is very sensitive with the change of β . Hence this decay is a promising channel to fix the β value once h_3^0 exists. On the other hand, $\text{Br}(h_3^0 \rightarrow hh)$ is sensitive with s_δ : it increases significantly with large s_δ , but the values is always small $\text{Br}(h_3^0 \rightarrow hh) < 1\%$.

For $m_F > m_{h_3^0}$ the total decay width of the h_3^0 gets mainly contribution from gluon decay channel, hence it is sensitive with only $m_{h_3^0}$ and v_3 , as given in Eq. (55). It is a bit sensitive with β , see illustrations in figure 11.

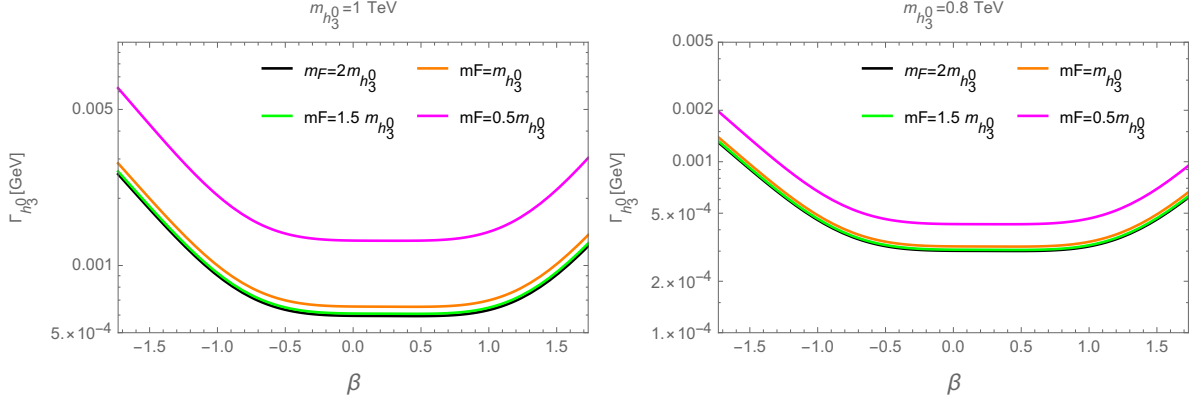


FIG. 11: Total decay width of h_3^0 as functions of β , where decays to exotic particle pairs do not included.

V. CONCLUSIONS

Significance of new physics predicted by the 3-3-1 models from the loop-induced neutral Higgs decays $h, h_3^0 \rightarrow \gamma\gamma, Z\gamma$ have been discussed. For the general case with arbitrary β , we have derived that these decays of the SM-like Higgs boson do not depend on the β , i.e., they cannot be used to distinguish different models corresponding to particular β values. This is because of the very large v_3 with values of around 10 TeV, leading to the suppressed one-loop contributions from heavy gauge and charged Higgs bosons, except the H^\pm , which are also predicted by the 2HDM and do not depend on β . Hence, the large deviations $\delta\mu_{Z\gamma, \gamma\gamma}$ will be originate from the one-loop contribution of the H^\pm and large $|s_\delta|$. In the region resulting in large $\delta\mu_{Z\gamma}$, the recent constrain on the significance of the di-photon decay always gives strict upper bound on that of the $h \rightarrow Z\gamma$ decay. In particular, our numerical investigation predicts $|\delta\mu_{Z\gamma}| \leq |\delta\mu_{\gamma\gamma}| < 0.23$, which is the sensitivity given in HC-HL project.

On the other hand, in a model with $\beta = \sqrt{3}$, where $v_3 \simeq 3$ TeV is still valid [74], $\delta\mu_{Z\gamma}$ may be large in the allowed region $\mu_{\gamma\gamma} = 0.99 \pm 0.14$. For the near future HC-HL project, where the experimental sensitivity for the decay $h \rightarrow \gamma\gamma$ may reach $|\delta\mu_{\gamma\gamma}| = 0.4$, this model still allows $|\delta\mu_{Z\gamma}|$ to be close to 0.1. But it cannot reach the near future sensitivity $|\delta\mu_{Z\gamma}| = 0.23$.

Theoretically, we have found two very interesting properties. First, $F_{21,sv}^{331}$ may have order of $F_{21,v}^{331}$ in allowed regions of the parameter space. This happens also in the 3-3-1 model with $\beta = \sqrt{3}$, where loop contribution from gauge and Higgs bosons may be large and have the same order. Hence, $F_{21,sv}^{331}$ must not be ignored as treatment for simplicity in previous works [34, 35]. Second, in the model with $\beta = \sqrt{3}$, one-loop contributions from gauge bosons

can reach the order of charged Higgs contributions, leading to that there appear regions that different contributions to the amplitude $h \rightarrow \gamma\gamma$ are destructive, while they are constructive in contributing to the decay amplitude $h \rightarrow Z\gamma$. This suggests that there may exist recent gauge extensions of the SM that allow large $\delta\mu_{Z\gamma}$ while still satisfy the future experimental data including $\delta\mu_{\gamma\gamma} \leq 0.04$.

On the other hand, the h_3^0 being the Higgs boson predicted by the $SU(3)_L$ symmetry, not appear in the effective 2HDM. This Higgs boson couples to only SM-like Higgs through the Higgs self couplings, while decouples to the remaining among the SM like particles. If h_3^0 is the lightest among new particles, loop-induced decays $h_3^0 \rightarrow \gamma\gamma, Z\gamma, gg$ are still allowed. Our investigation shows that the $\text{Br}(h \rightarrow \gamma\gamma)$ is very sensitive with the parameter β , hence it is a promising channel to distinguish different 3-3-1 models. Because of the strong Yukawa couplings with new heavy fermions, h_3^0 can be produced through the gluon fusion in the future project HL-LHC.

Acknowledgments

This research is funded by the Ministry of Education and Training of Vietnam under grant number: B.2018-SP2-12.

Appendix A: Heavy neutral Higgs couplings

From the Higgs potential and the aligned limit (26), the triple Higgs couplings containing one heavy neutral Higgs bosons are listed in table XIII. We only mention to the couplings relating with discussion on the decays $h_3^0 \rightarrow \gamma\gamma, Z\gamma$.

The non-zero couplings of heavy neutral Higgs bosons gauge bosons are listed in table XIV.

The couplings of Z to two exotic fermions are given in table XVI.

Vertex	Coupling: $-i\lambda_{S_i S_j S_k}$
$h_2^0 H^+ H^-$	$-i \left[2s_{12}c_{12}^2 (s_\alpha \lambda_1 + c_\alpha t_{12} \lambda_2) + (s_{12}^3 s_\alpha + c_{12}^3 c_\alpha) \lambda_{12} + s_\delta \tilde{\lambda}_{12} \right] v$
$h_2^0 H^A H^{-A}$	$-i \left[(2s_{12}s_\alpha \lambda_1 + c_\alpha c_{12}(\lambda_{12} + t_{13}^2 \lambda_{23})) + (2c_\alpha t_{12} + s_\alpha t_{13}^2) s_{12} \lambda_{13} + s_{12} s_\alpha \tilde{\lambda}_{13} \right] c_{13}^2 v$
$h_2^0 H^B H^{-B}$	$-i \left[(s_{12}s_\alpha \lambda_{12} + c_\alpha c_{12}(2\lambda_2 + t_{23}^2 \lambda_{23})) + (1 + c_{23}^2) s_\alpha s_{12} \lambda_{13} + c_{12} c_\alpha \tilde{\lambda}_{23} \right] c_{23}^2 v$
$h_3^0 H^+ H^-$	$-i \left[(1 + s_{12}^2) \lambda_{13} + s_{12}^2 \lambda_{23} \right] v_3$
$h_3^0 H^A H^{-A}$	$-i \left[2s_{13}^2 \lambda_3 + c_{13}^2 \lambda_{13} + \tilde{\lambda}_{13} \right] v_3$
$h_3^0 H^B H^{-B}$	$-i \left[2s_{23}^2 \lambda_3 + c_{23}^2 \lambda_{23} + \tilde{\lambda}_{23} \right] v_3$
h^3	$-i \left[2c_\alpha^3 s_{12} \lambda_1 - 2s_\alpha^3 c_{12} \lambda_2 + s_\alpha c_\alpha (s_\alpha s_{12} - c_\alpha c_{12}) \lambda_{12} \right] 3v$
$h^2 h_3^0$	$\frac{-i\lambda_{13}s_\delta^2 v_3}{c_{12}^2}$
$h h_2^0 h_3^0$	$i \frac{\lambda_{13}s_\delta c_\delta v_3}{c_{12}^2}$
$h h_3^0 h_3^0$	$-i \left[2c_\delta s_{12} - s_\delta c_{12}(t_{12}^2 - 1) \right] s_{12} \lambda_{13} v$
$h_2^0 h_3^0 h_3^0$	$-i \left[2s_\delta s_{12} + c_\delta c_{12}(t_{12}^2 - 1) \right] s_{12} \lambda_{13} v$
$h_3^0 h_3^0 h_3^0$	$-6i\lambda_3 v_3$

TABLE XIII: Triple Higgs couplings not included the CP-odd ones

Vertex	Coupling	Vertex	Coupling
$g_{h_2^0 W^+ W^-}$	$g m_W s_\delta$		
$g_{h_2^0 Y^+ A Y^- A}$	$g m_W s_{12} s_\alpha$	$g_{h_3^0 Y^+ A Y^- A}$	$\frac{g^2 v_3}{2}$
$g_{h_2^0 V^+ B V^- B}$	$g m_W c_{12} c_\alpha$	$g_{h_3^0 V^+ B V^- B}$	$\frac{g^2 v_3}{2}$
$g_{h_2^0 H W}$	$\frac{g c_\delta}{2}$	$g_{h_3^0 H W}$	0
$g_{h_2^0 H^- A Y^+ A}$	$-\frac{g c_{13} s_\alpha}{2}$	$g_{h_3^0 H^- A Y^+ A}$	$\frac{g s_{13}}{2}$
$g_{h_2^0 H^- B Y^+ B}$	$-\frac{g c_{23} c_\alpha}{2}$	$g_{h_3^0 H^- B Y^+ B}$	$\frac{g s_{23}}{2}$

TABLE XIV: Heavy neutral Higgs boson couplings to charged Higgs and gauge bosons.

Appendix B: Form factors to one-loop amplitudes of the neutral Higgs decays

$$h, h_3^0 \rightarrow Z \gamma \gamma$$

In the $331/\beta$ model, the explicit analytic formulas of one-loop contributions to the amplitudes of the decay $h \rightarrow \gamma\gamma, Z\gamma$ will be presented in terms of the Passarino-Veltmann (PV) functions [83], namely the one-loop three point PV functions denoted as C_i and C_{ij} with $i, j = 0, 1, 2$. The particular forms for one-loop contributions to the decay amplitudes

Vertex	coupling $g_{h_i^0 ZZ}$	
$h_1^0 ZZ$	$\frac{g_{m_W}}{c_W^2}$	$c_\delta \left(1 + \frac{2\sqrt{3}s_\theta c_\theta c_W (1-2s_{12}^2 - \sqrt{3}t_W^2 \beta)}{3\sqrt{1-\beta^2 t_W^2}} \right) - \frac{4s_\delta c_W s_\theta c_\theta s_{12} c_{12}}{\sqrt{3(1-\beta^2 t_W^2)}} \right)$
$h_2^0 ZZ$	$\frac{g_{m_W}}{c_W^2}$	$s_\delta \left(1 + \frac{2\sqrt{3}s_\theta c_\theta c_W (1-2s_{12}^2 - \sqrt{3}t_W^2 \beta)}{3\sqrt{1-\beta^2 t_W^2}} \right) + \frac{4c_\delta c_W s_\theta c_\theta s_{12} c_{12}}{\sqrt{3(1-\beta^2 t_W^2)}} \right)$

TABLE XV: $h_i^0 ZZ$ couplings in the limit $s_\theta^2 = 0$, $c_\theta^2 = 1$.

F	g_L^F	g_R^F
E_a	$g_R^{E_a} - \frac{t_\theta c_W}{\sqrt{3(1-\beta^2 t_W^2)}}$	$-\frac{(-1+\sqrt{3}\beta)s_W^2}{2} \left(1 - \frac{t_\theta \beta}{c_W \sqrt{1-\beta^2 t_W^2}} \right)$
J_i	$g_R^{J_i} + \frac{t_\theta c_W}{\sqrt{3(1-\beta^2 t_W^2)}}$	$\frac{(-1+3\sqrt{3}\beta)s_W^2}{6} \left(1 - \frac{t_\theta \beta}{c_W \sqrt{1-\beta^2 t_W^2}} \right)$
J_3	$g_R^{J_3} - \frac{t_\theta c_W}{\sqrt{3(1-\beta^2 t_W^2)}}$	$-\frac{(1+3\sqrt{3}\beta)s_W^2}{6} \left(1 - \frac{t_\theta \beta}{c_W \sqrt{1-\beta^2 t_W^2}} \right)$

TABLE XVI: Couplings of Z with exotic fermions

$h \rightarrow Z\gamma, \gamma\gamma$ were given in Ref. [45], which are consistent with the previous formulas [44]. We have used the LoopTools [84] to evaluate numerical results.

For the loop-induced decays of the heavy neutral Higgs bosons h_3^0 , the calculation is the same way as those for the SM-like Higgs boson h . Correspondingly, the mass and couplings of h are replaced with those relating with h_3^0 . The h_2^0 properties were discussed in ref. [1], we do not repeat again.

The contributions from the SM fermions corresponding to the diagram 1 in Fig. 1 are

$$F_{21,f}^{331} = -\frac{e Q_f N_c}{4\pi^2} \left[m_f Y_{h\bar{f}fL} \frac{g_{c_\theta}}{c_W} \left(g_L^f + g_R^f \right) \right] [4(C_{12} + C_{22} + C_2) + C_0], \quad (B1)$$

where $C_{0,i,ij} \equiv C_{0,i,ij}(m_Z^2, 0, m_h^2; m_f^2, m_f^2, m_f^2)$; Q_f , N_c and m_f are respectively the electric charge, color factor and mass of the SM fermions. The factors $Y_{h\bar{f}fL}$ and $g_{L,R}^f$ are listed in tables I and V, respectively.

The contributions from the charged Higgs bosons $s = H^\pm, H^{\pm A}, H^{\pm B}$ corresponding to the diagram 2 in Fig. 1 are

$$F_{21,s}^{331} = \frac{e Q_s \lambda_{hss} g_{Zss}}{2\pi^2} [C_{12} + C_{22} + C_2], \quad (B2)$$

where $s = H^\pm, H^{\pm A}, H^{\pm B}$, $C_{0,i,ij} \equiv C_{0,i,ij}(m_Z^2, 0, m_h^2; m_s^2, m_s^2, m_s^2)$, and the couplings λ_{hss}, g_{Zss} are listed in table I and IV.

The contributions from the diagrams containing both charged Higgs and gauge bosons $\{v, s\} = \{W^\pm, H^\pm\}, \{Y^{\pm A}, H^{\pm A}\}, \{V^{\pm B}, H^{\pm B}\}$ corresponding to the two diagrams 3 and 4

in Fig. 1 are

$$F_{21,vss}^{331} = \frac{e Q_s g_{hvs} g_{Zvs}}{4\pi^2} \left[\left(1 + \frac{-m_s^2 + m_h^2}{m_v^2} \right) (C_{12} + C_{22} + C_2) + 2(C_1 + C_2 + C_0) \right], \quad (\text{B3})$$

$$F_{21,svv}^{331} = \frac{e Q_v g_{hvs} g_{Zvs}}{4\pi^2} \left[\left(1 + \frac{-m_s^2 + m_h^2}{m_v^2} \right) (C_{12} + C_{22} + C_2) - 2(C_1 + C_2) \right], \quad (\text{B4})$$

where $C_{0,i,ij} \equiv C_{0,i,ij}(m_Z^2, 0, m_h^2; m_V^2, m_s^2, m_s^2)$ or $C_{0,i,ij}(m_Z^2, 0, m_h^2; m_s^2, m_V^2, m_V^2)$ corresponding to Eqs. (B3) or (B4). The vertex factors are listed in table III and IV.

The contributions from the charged gauge bosons $v = W^\pm, Y^{\pm A}, V^{\pm B}$ corresponding to the diagram 5 in Fig. 1 are

$$F_{21,v}^{331} = \frac{e Q_v g_{hvv} g_{Zvv}}{8\pi^2} \times \left\{ \left[8 + \left(2 + \frac{m_h^2}{m_v^2} \right) \left(2 - \frac{m_Z^2}{m_v^2} \right) \right] (C_{12} + C_{22} + C_2) + 2 \left(4 - \frac{m_Z^2}{m_v^2} \right) C_0 \right\}, \quad (\text{B5})$$

where $v = W^\pm, Y^{\pm A}, V^{\pm B}$, $C_{0,i,ij} \equiv C_{0,i,ij}(m_Z^2, 0, m_h^2; m_v^2, m_v^2, m_v^2)$. The vertex factors are listed in table III and VI.

For the decay $h \rightarrow \gamma\gamma$, analytic formulas of F_γ^{331} can be derived from the F_{21}^{331} by taking replacements $g_{Zvv}, g_{Zss}, \frac{gc_0}{c_W} g_{L,R}^f \rightarrow eQ_v, eQ_s, eQ_f$ and the respective PV functions, name ly:

$$\begin{aligned} F_{\gamma\gamma,f}^{331} &= -\frac{e^2 Q_f^2 N_c}{2\pi^2} (m_f Y_{h\bar{f}fL}) [4(C_{12} + C_{22} + C_2) + C_0], \\ F_{\gamma\gamma,s}^{331} &= \frac{e^2 Q_s^2 \lambda_{hss}}{2\pi^2} [C_{12} + C_{22} + C_2], \\ F_{\gamma\gamma,v}^{331} &= \frac{e^2 Q_V^2 g_{hvv}}{4\pi^2} \times \left\{ \left(6 + \frac{m_h^2}{m_V^2} \right) (C_{12} + C_{22} + C_2) + 4C_0 \right\}, \end{aligned} \quad (\text{B6})$$

where $C_{0,i,ij} \equiv C_{0,i,ij}(0, 0, m_h^2; m_x^2, m_x^2, m_x^2)$ with $x = f, s, v$ corresponding to the contribution from fermions, charged Higgs and gauge bosons.

Regarding to h_3^0 , we emphasize again that the only non-zero coupling with SM particle is the triple couplings with two SM-like Higgs bosons. Hence the fermion contributions to the decay amplitudes $h_3^0 \rightarrow \gamma\gamma, Z\gamma, gg$ are only exotic fermions $F = E_a, J_a$. These contributions are denoted as $F_{\gamma\gamma,F}^{331,h_3^0}, F_{21,F}^{331,h_3^0}, F_{gg,F}^{331,h_3^0}$. They are derived base on Eq. (42) with the following replacement,

$$\begin{aligned} F_{21,F}^{331}(h_3^0 \rightarrow Z\gamma) &= F_{21,f}^{331}(f \rightarrow F, h \rightarrow h_3^0), \\ F_{\gamma\gamma,F}^{331}(h_3^0 \rightarrow Z\gamma) &= F_{\gamma\gamma,f}^{331}(f \rightarrow F, h \rightarrow h_3^0). \end{aligned} \quad (\text{B7})$$

The other contributions to the mentioned h_3^0 decays are calculated by simple replacements the mass and couplings of the SM-like Higgs bosons with those of the h_3^0 . We note that the W bosons does not included in these amplitudes.

Appendix C: More numerical illustrations discussed in section IV

Contour plots with other numerical values of.

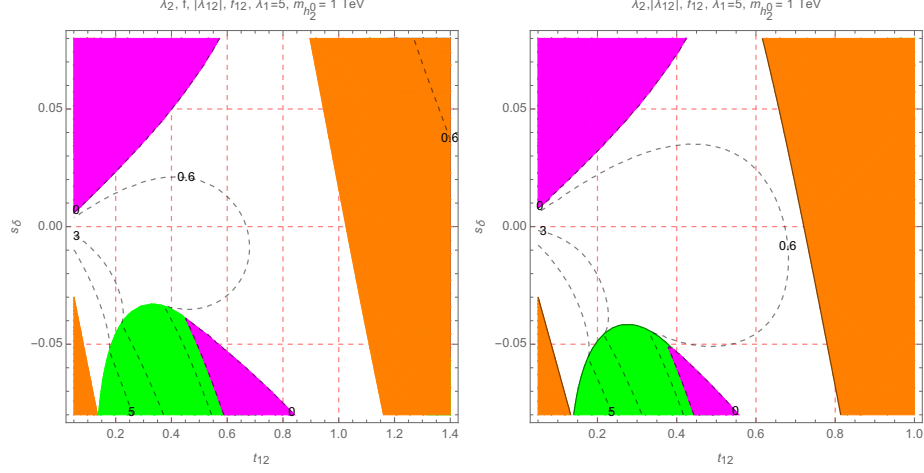


FIG. 12: Contour plots of λ_2 , $|\lambda_{12}|$ and f_{12} as functions of s_δ and t_{12} . The green, orange, magenta regions are excluded by requirements that $0 < \lambda_2 < 10$, $|\lambda_{12}| < 10$, and $f_{12} > 0$, respectively

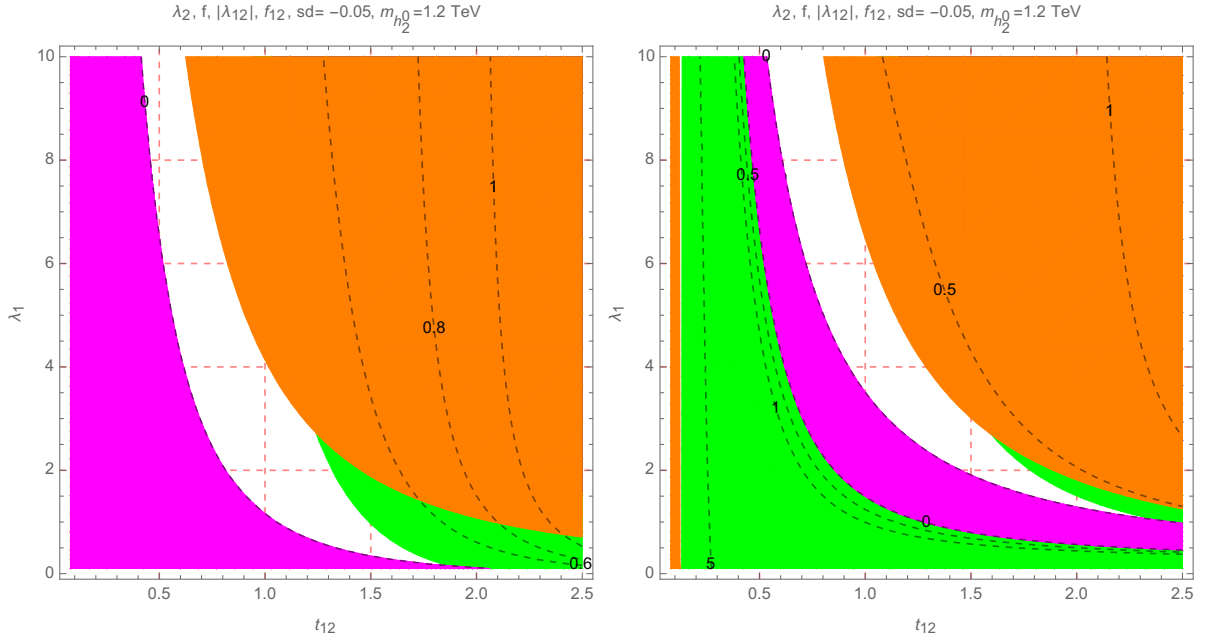


FIG. 13: Contour plots of λ_2 , $|\lambda_{12}|$ and f_{12} as functions of λ_1 and t_{12} with some fixed $m_{h_2^0}$. The green, orange, magenta regions are excluded by requirements that $0 < \lambda_2 < 10$, $|\lambda_{12}| < 10$, and $f_{12} > 0$, respectively

-
- [1] H. Okada, N. Okada, Y. Orikasa and K. Yagyu, Phys. Rev. D **94** (2016), 015002 [arXiv:1604.01948 [hep-ph]].
 - [2] M. Aaboud *et al.* [ATLAS Collaboration], Phys. Lett. B **786** (2018) 114 [arXiv:1805.10197 [hep-ex]].
 - [3] A. M. Sirunyan *et al.* [CMS Collaboration], JHEP **1811** (2018) 185 [arXiv:1804.02716 [hep-ex]].
 - [4] M. Aaboud *et al.* [ATLAS Collaboration], Phys. Rev. D **98** (2018) 052005 [arXiv:1802.04146 [hep-ex]].
 - [5] S. Heinemeyer *et al.* [LHC Higgs Cross Section Working Group], doi:10.5170/CERN-2013-004 arXiv:1307.1347 [hep-ph].
 - [6] D. de Florian *et al.* [LHC Higgs Cross Section Working Group], arXiv:1610.07922 [hep-ph].
 - [7] M. Aaboud *et al.* [ATLAS Collaboration], JHEP **1710** (2017) 112 [arXiv:1708.00212 [hep-ex]].
 - [8] A. M. Sirunyan *et al.* [CMS Collaboration], JHEP **1811** (2018) 152 [arXiv:1806.05996 [hep-ex]].
 - [9] M. Cepeda *et al.* [Physics of the HL-LHC Working Group], “Higgs Physics at the HL-LHC and HE-LHC,” arXiv:1902.00134 [hep-ph].
 - [10] D. Fontes, J. C. Romo and J. P. Silva, JHEP **1412** (2014) 043 [arXiv:1408.2534 [hep-ph]].
 - [11] S. Kanemura, M. Kikuchi, K. Mawatari, K. Sakurai and K. Yagyu, Phys. Lett. B **783** (2018) 140 [arXiv:1803.01456 [hep-ph]].
 - [12] T. Bandyopadhyay, D. Das, R. Pasechnik and J. Rathsmann, Phys. Rev. D **99** (2019) no.11, 115021 [arXiv:1902.03834 [hep-ph]].
 - [13] R. Martinez, M. A. Perez and J. J. Toscano, Phys. Lett. B **234** (1990) 503.
 - [14] A. Maiezza, M. Nemevek and F. Nesti, Phys. Rev. D **94** (2016) no.3, 035008 [arXiv:1603.00360 [hep-ph]].
 - [15] C. H. Chen and T. Nomura, “Radiatively scotogenic type-II seesaw and a relevant phenomenological analysis,” arXiv:1906.10516 [hep-ph].
 - [16] S. Blunier, G. Cottin, M. A. Daz and B. Koch, Phys. Rev. D **95** (2017) no.7, 075038 [arXiv:1611.07896 [hep-ph]].
 - [17] S. Kanemura, K. Mawatari and K. Sakurai, Phys. Rev. D **99** (2019) no.3, 035023

- [arXiv:1808.10268 [hep-ph]].
- [18] M. Singer, J. W. F. Valle and J. Schechter, Phys. Rev. D **22** (1980) 738.
 - [19] J. W. F. Valle and M. Singer, Phys. Rev. D **28** (1983) 540.
 - [20] F. Pisano and V. Pleitez, Phys. Rev. D **46** (1992) 410 [hep-ph/9206242].
 - [21] R. Foot, O. F. Hernandez, F. Pisano and V. Pleitez, Phys. Rev. D **47** (1993) 4158 [hep-ph/9207264].
 - [22] P. H. Frampton, Phys. Rev. Lett. **69** (1992) 2889.
 - [23] R. Foot, H. N. Long and T. A. Tran, Phys. Rev. D **50** (1994) no.1, R34 [hep-ph/9402243].
 - [24] C. A. de Sousa Pires and O. P. Ravinez, Phys. Rev. D **58** (1998) 035008 [Phys. Rev. D **58** (1998) 35008] [hep-ph/9803409].
 - [25] J. C. Montero, V. Pleitez and O. Ravinez, Phys. Rev. D **60** (1999) 076003 [hep-ph/9811280].
 - [26] J. C. Montero, C. C. Nishi, V. Pleitez, O. Ravinez and M. C. Rodriguez, Phys. Rev. D **73** (2006) 016003 [hep-ph/0511100].
 - [27] P. B. Pal, Phys. Rev. D **52** (1995) 1659 [hep-ph/9411406].
 - [28] A. G. Dias, V. Pleitez and M. D. Tonasse, Phys. Rev. D **67** (2003) 095008 [hep-ph/0211107].
 - [29] A. G. Dias and V. Pleitez, Phys. Rev. D **69** (2004) 077702 [hep-ph/0308037].
 - [30] A. G. Dias, C. A. de S. Pires and P. S. Rodrigues da Silva, Phys. Rev. D **68** (2003) 115009 [hep-ph/0309058].
 - [31] L. T. Hue and L. D. Ninh, Mod. Phys. Lett. A **31** (2016) no.10, 1650062 [arXiv:1510.00302 [hep-ph]].
 - [32] E. Ramirez Barreto and D. Romero Abad, “Heavy long-lived fractionally charged leptons in novel $3 - 3 - 1$ model,” arXiv:1907.02613 [hep-ph].
 - [33] A. J. Buras and F. De Fazio, JHEP **1608** (2016) 115 [arXiv:1604.02344 [hep-ph]].
 - [34] Q. H. Cao and D. M. Zhang, “Collider Phenomenology of the 3-3-1 Model,” arXiv:1611.09337 [hep-ph].
 - [35] C. X. Yue, Q. Y. Shi and T. Hua, Nucl. Phys. B **876** (2013) 747 [arXiv:1307.5572 [hep-ph]]; W. Caetano, C. A. de S. Pires, P. S. Rodrigues da Silva, D. Cogollo and F. S. Queiroz, Eur. Phys. J. C **73** (2013) no.10, 2607 [arXiv:1305.7246 [hep-ph]].
 - [36] L. T. Hue, L. D. Ninh, T. T. Thuc and N. T. T. Dat, Eur. Phys. J. C **78** (2018) no.2, 128 [arXiv:1708.09723 [hep-ph]].
 - [37] A. E. Carcamo Hernandez, R. Martinez and F. Ochoa, Phys. Rev. D **73** (2006) 035007 [hep-

- ph/0510421].
- [38] A. J. Buras, F. De Fazio and J. Girrbach, JHEP **1402** (2014) 112 [arXiv:1311.6729 [hep-ph]].
 - [39] R. Martinez and F. Ochoa, Phys. Rev. D **90** (2014) no.1, 015028 [arXiv:1405.4566 [hep-ph]].
 - [40] H. N. Long, N. V. Hop, L. T. Hue and N. T. T. Van, Nucl. Phys. B **943** (2019) 114629 [arXiv:1812.08669 [hep-ph]].
 - [41] A. J. Buras, F. De Fazio and J. Girrbach-Noe, JHEP **1408** (2014) 039 [arXiv:1405.3850 [hep-ph]].
 - [42] W. Caetano, C. A. de S. Pires, P. S. Rodrigues da Silva, D. Cogollo and F. S. Queiroz, Eur. Phys. J. C **73** (2013) no.10, 2607 [arXiv:1305.7246 [hep-ph]].
 - [43] A. E. Crcamo Hernndez, Y. H. Velsquez and N. A. Prez-Julve, “A 3-3-1 model with low scale seesaw mechanisms,” arXiv:1905.02323 [hep-ph].
 - [44] C. Degrande, K. Hartling and H. E. Logan, Phys. Rev. D **96** (2017) no.7, 075013 Erratum: [Phys. Rev. D **98** (2018) no.1, 019901] [arXiv:1708.08753 [hep-ph]].
 - [45] L. T. Hue, A. B. Arbuzov, T. T. Hong, T. P. Nguyen, D. T. Si and H. N. Long, Eur. Phys. J. C **78** (2018) no.11, 885 [arXiv:1712.05234 [hep-ph]].
 - [46] U. Haisch and G. Polesello, JHEP **1809** (2018) 151 doi:10.1007/JHEP09(2018)151 [arXiv:1807.07734 [hep-ph]].
 - [47] S. Descotes-Genon, M. Moscati and G. Ricciardi, Phys. Rev. D **98** (2018) no.11, 115030 [arXiv:1711.03101 [hep-ph]].
 - [48] L. T. Hue and L. D. Ninh, Eur. Phys. J. C **79** (2019) no.3, 221 [arXiv:1812.07225 [hep-ph]].
 - [49] N. Craig and S. Thomas, JHEP **1211** (2012) 083 [arXiv:1207.4835 [hep-ph]].
 - [50] A. J. Buras, F. De Fazio, J. Girrbach, and M. V. Carlucci, JHEP **02**, 023 (2013), arXiv:1211.1237.
 - [51] B. L. Snchez-Vega, G. Gambini and C. E. Alvarez-Salazar, Eur. Phys. J. C **79** (2019) no.4, 299 [arXiv:1811.00585 [hep-ph]].
 - [52] K. Huitu and N. Koivunen, “Suppression of scalar mediated FCNCs in a $SU(3)_c \times SU(3)_L \times U(1)_X$ -model,” arXiv:1905.05278 [hep-ph].
 - [53] R. A. Diaz, R. Martinez and F. Ochoa, Phys. Rev. D **72**, 035018 (2005) [hep-ph/0411263].
 - [54] J. F. Gunion, H. E. Haber, G. L. Kane and S. Dawson, “The Higgs Hunter’s Guide,” Front. Phys. **80** (2000) 1.
 - [55] M. Tanabashi *et al.* [Particle Data Group], Phys. Rev. D **98** (2018) no.3, 030001.

- [56] G. Aad *et al.* [ATLAS and CMS Collaborations], JHEP **1608** (2016) 045 [arXiv:1606.02266 [hep-ex]].
- [57] S. Banerjee and N. Chakrabarty, “A revisit to scalar dark matter with radiative corrections,” arXiv:1612.01973 [hep-ph].
- [58] S. De Lope Amigo, W. M. Y. Cheung, Z. Huang and S. P. Ng, JCAP **0906** (2009) 005 [arXiv:0812.4016 [hep-ph]].
- [59] B. Eiteneuer, A. Goudelis and J. Heisig, Eur. Phys. J. C **77** (2017) no.9, 624 [arXiv:1705.01458 [hep-ph]].
- [60] A. Belyaev, G. Cacciapaglia, I. P. Ivanov, F. Rojas-Abatte and M. Thomas, Phys. Rev. D **97** (2018) no.3, 035011 [arXiv:1612.00511 [hep-ph]].
- [61] S. Filippi, W. A. Ponce and L. A. Sanchez, Europhys. Lett. **73** (2006) 142 [hep-ph/0509173].
- [62] D. Cogollo, A. X. Gonzalez-Morales, F. S. Queiroz and P. R. Teles, JCAP **1411** (2014) no.11, 002 [arXiv:1402.3271 [hep-ph]].
- [63] C. A. de S.Pires and P. S. Rodrigues da Silva, JCAP **0712** (2007) 012 [arXiv:0710.2104 [hep-ph]].
- [64] S. M. Boucenna, A. Celis, J. Fuentes-Martin, A. Vicente and J. Virto, JHEP **1612** (2016) 059 [arXiv:1608.01349 [hep-ph]].
- [65] M. Spira, Fortsch. Phys. **46** (1998) 203 [hep-ph/9705337].
- [66] Y. A. Coutinho, V. Salustino Guimares and A. A. Nepomuceno, Phys. Rev. D **87** (2013) no.11, 115014 [arXiv:1304.7907 [hep-ph]].
- [67] M. M. Ferreira, T. B. de Melo, S. Kovalenko, P. R. D. Pinheiro and F. S. Queiroz, “Lepton Flavor Violation and Collider Searches in a Type I + II Seesaw Model,” arXiv:1903.07634 [hep-ph].
- [68] H. N. Long, N. V. Hop, L. T. Hue, N. H. Thao and A. E. Carcamo Hernandez, Phys. Rev. D **100**, No 1, 015004 (2019) [arXiv:1810.00605 [hep-ph]].
- [69] M. Aaboud *et al.* [ATLAS Collaboration], JHEP **1801** (2018) 055 [arXiv:1709.07242 [hep-ex]].
- [70] A. M. Sirunyan *et al.* [CMS Collaboration], JHEP **1806** (2018) 120 doi:10.1007/JHEP06(2018)120 [arXiv:1803.06292 [hep-ex]].
- [71] G. Aad *et al.* [ATLAS Collaboration], “Search for high-mass dilepton resonances using 139 fb⁻¹ of *pp* collision data collected at $\sqrt{s}=13$ TeV with the ATLAS detector,” arXiv:1903.06248 [hep-ex].

- [72] F. F. Freitas, C. A. de S. Pires and P. Vasconcelos, Phys. Rev. D **98** (2018) no.3, 035005 [arXiv:1805.09082 [hep-ph]].
- [73] G. Arcadi, M. Lindner, J. Martins and F. S. Queiroz, “New Physics Probes: Atomic Parity Violation, Polarized Electron Scattering and Neutrino-Nucleus Coherent Scattering,” arXiv:1906.04755 [hep-ph].
- [74] G. Corcella, C. Corian, A. Costantini and P. H. Frampton, Phys. Lett. B **785** (2018) 73 [arXiv:1806.04536 [hep-ph]].
- [75] S. Kanemura, T. Kasai and Y. Okada, Phys. Lett. B **471** (1999) 182 [hep-ph/9903289].
- [76] G. Aad *et al.* [ATLAS Collaboration], JHEP **1511** (2015) 206 [arXiv:1509.00672 [hep-ex]].
- [77] J. Haller, A. Hoecker, R. Kogler, K. Mnig, T. Peiffer and J. Stelzer, Eur. Phys. J. C **78** (2018) no.8, 675 [arXiv:1803.01853 [hep-ph]].
- [78] P. M. Ferreira, M. Mhlleitner, R. Santos, G. Weiglein and J. Wittbrodt, “Vacuum Instabilities in the N2HDM,” arXiv:1905.10234 [hep-ph].
- [79] K. Kainulainen, V. Keus, L. Niemi, K. Rummukainen, T. V. I. Tenkanen and V. Vaskonen, JHEP **1906** (2019) 075 [arXiv:1904.01329 [hep-ph]].
- [80] K. S. Babu and S. Jana, JHEP **1902** (2019) 193 [arXiv:1812.11943 [hep-ph]].
- [81] M. Aaboud *et al.* [ATLAS Collaboration], Eur. Phys. J. C **78** (2018) no.1, 24 [arXiv:1710.01123 [hep-ex]].
- [82] A. G. Dias and V. Pleitez, Phys. Rev. D **80** (2009) 056007 [arXiv:0908.2472 [hep-ph]].
- [83] G. Passarino and M. J. G. Veltman, Nucl. Phys. B **160** (1979) 151.
- [84] T. Hahn and M. Perez-Victoria, Comput. Phys. Commun. **118** (1999) 153 [hep-ph/9807565].
- [85] A. Palcu, “On trilinear terms in the scalar potential of 3-3-1 gauge models,” arXiv:1907.00572 [hep-ph].
- [86] V. Khachatryan *et al.* [CMS Collaboration], Eur. Phys. J. C **74** (2014) no.10, 3076 [arXiv:1407.0558 [hep-ex]].
- [87] G. Aad *et al.* [ATLAS Collaboration], Phys. Rev. D **90** (2014) no.11, 112015 [arXiv:1408.7084 [hep-ex]].
- [88] L. T. Hue, A. B. Arbuzov, N. T. K. Ngan and H. N. Long, Eur. Phys. J. C **77** (2017) no.5, 346 [arXiv:1611.06801 [hep-ph]].
- [89] X. G. He and G. Valencia, Phys. Lett. B **779** (2018) 52 [arXiv:1711.09525 [hep-ph]].
- [90] M. Abdullah, J. Calle, B. Dutta, A. Flrez and D. Restrepo, Phys. Rev. D **98** (2018) no.5,

055016 [arXiv:1805.01869 [hep-ph]].

[91] C. X. Yue and S. S. Jia, J. Phys. G **46** (2019) no.7, 075001.